

Supporting Information

DNA-Origami-Based Fluorescence Brightness Standards for Convenient and Fast Protein Counting in Live Cells

Nathan D. Williams^{1,2}, Ane Landajuela^{2,3}, Ravi Kiran Kasula¹, Wenjiao Zhou^{1,2,†}, John T. Powell^{1,2}, Zhiqun Xi¹, Farren J. Isaacs^{4,5,6}, Julien Berro^{1,2,7}, Derek Toomre¹, Erdem Karatekin^{2,3,7,8}, Chenxiang Lin^{1,2,*}

¹ Department of Cell Biology, Yale University School of Medicine, New Haven, CT 06520, USA

² Nanobiology Institute, Yale University, West Haven CT 06516, USA

³ Department of Cellular and Molecular Physiology, Yale University School of Medicine, New Haven, CT 06520, USA

⁴ Department of Molecular, Cellular and Developmental Biology, Yale University, New Haven, CT 06520, USA

⁵ Department of Biomedical Engineering, Yale University, New Haven, CT 06520, USA

⁶ Systems Biology Institute, Yale University, West Haven, CT 06516, USA

⁷ Department of Molecular Biophysics and Biochemistry, New Haven, CT 06520, USA

⁸ Université de Paris, SPPIN – Saints-Pères Paris Institute for the Neurosciences, Centre National de la Recherche Scientifique (CNRS), F-75006 Paris, France

† Present address: College of Chemistry and Chemical Engineering, Chongqing University of Technology, Chongqing, China

* Email: chenxiang.lin@yale.edu

Table of Contents

Materials and Methods	3
Materials	3
Agarose gel electrophoresis	3
SDS-polyacrylamide gel electrophoresis (SDS-PAGE)	3
DNA-origami structure design.....	3
DNA-origami structure folding and purification	3
DNA-origami structure dimerization	4
Fluorescently labeling DNA-origami structures	4
mEGFP standard purification.....	4
Transmission electron microscopy.....	4
SiR standard purification.....	4
mEGFP-pAzF cloning	5
GRO transformation.....	5
mEGFP-pAzF overexpression	5
mEGFP(pAzF) His-trap FPLC purification	5
mEGFP – alkyne DNA conjugation and purification	6
SiR-azide – alkyne-DNA click reaction	6
Urea-PAGE Purification of SiR-DNA conjugate.	6
Generation of <i>B. subtilis</i> cells expressing dnaC-mEGFP	7
Imaging of mEGFP standards and <i>B. subtilis</i> cells	7
Image processing of wide-field microscopy images.....	8
CLC (Clathrin Light Chain)-HaloTag CRISPR/Cas9 gene editing.....	8
CLC-Halo cell cultures	8
CLC-Halo labeling with SiR-chloroalkane (SiR-CA) in HeLa cells	8
Imaging SiR standards and SiR labeled CLC-Halo in HeLa cells	9
Image processing of confocal micrographs	9
Supplementary Figures	10
Figure S1. Diagrams of mEGFP standards	10
Figure S2. Diagrams of SiR standards	10
Figure S3. Distances between fluorophores	11
Figure S4. Design (caDNAo) diagrams of DNA-origami nanotubes.	12
Figure S5. mEGFP in-gel fluorescence recovery.....	13
Figure S6. mEGFP-DNA conjugates after anion-exchange purification.....	14

Figure S7. mEGFP-DNA conjugates after size-exclusion purification.....	15
Figure S8. Purified mEGFP-DNA conjugates.	15
Figure S9. mEGFP standards electrophoresed in an agarose gel.....	16
Figure S10. Test for mEGFP self-quenching	16
Figure S11. TEM micrographs of mEGFP standards.....	17
Figure S12. Wide-field fluorescence micrographs of mEGFP standards.....	18
Figure S13. Wide-field fluorescence micrographs of <i>B. subtilis</i>	19
Figure S14. Image processing pipeline for mEGFP labeling	20
Figure S15. Handle occupancy estimation	21
Figure S16. SiR-DNA conjugate analyzed by PAGE	22
Figure S17. Fluorescent barcode pattern on 25× SiR standard	23
Figure S18. Fluorescent barcode pattern on 50× SiR standard	24
Figure S19. Fluorescent barcode pattern on 100× SiR standard.....	25
Figure S20. Fluorescent barcode pattern on 150× SiR standard.....	26
Figure S21. Fluorescent barcode pattern on 200× SiR standard.....	27
Figure S22. Confocal fluorescence micrographs of SiR standards.....	28
Figure S23. A confocal fluorescence micrograph of HeLa cells.....	29
Figure S24. Image processing pipeline for SiR labeling	30
Figure S25. Stability of DNA-origami standards in imaging media	31
Figure S26. Multiple DNA-origami barcodes imaged together.....	32
Supplementary Tables	33
Table S1: Handle and antihandle sequences	33
Table S2: Linker DNA strands used in dimers	33
Table S3: DNA-origami-assisted quantitative fluorescence microscopy methods	34
Table S4: Imaging parameters	34
Supplementary References.....	35

Materials and Methods

Materials

DNA oligonucleotides were synthesized by Integrated DNA Technologies. All chemical reagents were purchased from Millipore Sigma unless otherwise specified. Enzymes were purchased from New England Biolabs unless otherwise specified. Water is purified by a Milli-Q (Millipore) system.

Agarose gel electrophoresis

Unless otherwise indicated, all agarose gels contained 1.5% agarose, and were run in 0.5×TBE + 10 mM MgCl₂ for 3 hrs at 5V/cm at room temperature. Gels were imaged on a Typhoon FLA 9500 scanner. Whenever necessary, gels were stained with Ethidium Bromide (EtBr, 0.5 µg/mL) after imaging any other relevant channels (for fluorescent labels on DNA-origami structures).

SDS-polyacrylamide gel electrophoresis (SDS-PAGE)

Unless otherwise indicated, all gels contained 12% acrylamide bis-tris (Bio-Rad), and were run for 45 minutes at 200 V in 1× SDS MOPS buffer (50 mM Tris base, 50 mM MOPS, 1 mM EDTA, 0.1% SDS, pH 6.5). Samples were prepared in 30% glycerol supplemented with orange G dye, and were heated 5 minutes at 95°C before loading. In gels where mEGFP was imaged, SDS was first rinsed away by three 20-minute washes in water. We found this protocol was able to recover mEGFP fluorescence sufficiently to image (See Figure S5).

SYBR Gold staining was performed by submerging gels in SYBR Gold stain (Invitrogen) diluted 10,000× in water, per manufacturer recommendations. Gels were briefly rinsed with water before imaging on a Typhoon FLA 9500 scanner.

Coomassie staining was performed by submerging gels in 1× Coomassie solution (50% methanol, 10% glacial acetic acid, 0.1% w/v Coomassie blue) and microwaving on high until boiling (approximately 1 minute). Gels were then briefly rinsed with water, covered in Coomassie destain solution (12% methanol, 7% glacial acetic acid), and microwaved on high until boiling (approximately 1 minute). Containers with gels heated in destain solution were then placed on a platform shaker, and Kimwipes were added to speed Coomassie desorption. Gels were checked approximately every 30 minutes until clear enough to be imaged. Coomassie-stained gels were imaged on a transilluminator (Bio-Rad) with white light. In cases where multiple scans were used, gels were imaged and stained in the following order: in-gel fluorophores (e.g. mEGFP), SYBR Gold, and Coomassie.

DNA-origami structure design

DNA-origami six-helix bundle (6hb) nanotubes were designed using caDNAno (cadnano.org)¹. Design diagrams are shown in Figure S4. Orthogonal handle sequences were generated using NUPACK (nupack.org) and added to the 3'-ends of selected staple strands. Handle sequences are shown in Table S1.

DNA-origami structure folding and purification

DNA origami folding mixtures were prepared by adding 6× molar excess of staple strands to p7308 scaffold² in 1×TE buffer (25 mM Tris•HCl, 1 mM EDTA•Na₂, pH 8) supplemented with 10 mM MgCl₂. Mixtures were heated in a thermocycler (Bio-Rad) to 85°C for 3 min, cooled from 80°C to 60°C in 80 minutes, 60°C to 24°C in 15 hours, and then held at 4°C. Excess staples were removed by PEG precipitation and re-suspending pellets in 1×TE buffer + 10 mM MgCl₂.³

DNA-origami structure dimerization

“Front” and “rear” monomeric halves of dimeric nanotubes were folded independently and PEG precipitated to remove excess staples (see above). Concentrations of purified monomers were estimated by absorbance, and equimolar amounts of each half were mixed in 1×TE buffer + 10 mM MgCl₂ with 10× molar excess of linker strands (Table S2). These dimer mixtures were heated to 55°C and cooled to 20°C over 18 hours.

Fluorescently labeling DNA-origami structures

To add antihandles to DNA nanotubes, a molar excess of antihandle was added to origami in 1×TE buffer + 10 mM MgCl₂: 3× excess for mEGFP and SiR antihandles, and 1.2× excess in the case of other antihandles. 3× excess was used to maximize antihandle attachment for the most important fluorophores. The mixture is incubated at 37°C for 2 hours. In the case of dimeric structures, linker DNA was kept at 10× molar excess during the labeling step. The labeled DNA-origami dimers were then purified by rate-zonal centrifugation (see below).

mEGFP standard purification

DNA-origami nanotubes labeled by mEGFP and Alexa Fluor 647 were PEG precipitated to remove excess antihandles. Briefly, a equal volume of 2×PEG-precipitation buffer (1×TE, 15% PEG, 10 mM MgCl₂, 500 mM NaCl, pH 8) was added to the hybridization mixture (DNA nanotubes + labeled-antihandles), and the mixture was spun at 16,000-g for 25 minutes at 4°C. The pellet was then resuspended in 1×TE + 10 mM MgCl₂. A typical preparation starting with 45 μL of 4 nM unlabeled DNA nanotubes yields 45 μL of 2.7 nM purified mEGFP-labeled DNA nanotubes, over 67% recovery.

Transmission electron microscopy

For negative-stain TEM, a drop of the sample (5 μL) was deposited on a glow discharged formvar/carbon-coated copper grid (Electron Microscopy Sciences), incubated for 1 min, and blotted away. The grid was first rinsed twice with 1× TE buffer + 10 mM MgCl₂, then washed briefly and stained for 1 min with 2% (w/v) uranyl formate. Images were acquired on a JEOL JEM-1400Plus microscope (acceleration voltage: 80 kV) with a bottom-mount 4k×3k CCD camera (Advanced Microscopy Technologies).

SiR standard purification

Dimeric DNA-origami nanotubes labeled with fluorophores and biotin were purified by rate-zonal centrifugation over a glycerol gradient⁴. Gradients were 15%–45% glycerol in 1×TE buffer supplemented with 10 mM MgCl₂, and were spun at 48k RPM for 1.5 hrs at 4°C. Fractions were subsequently collected and run in agarose gels to find the fractions

containing properly labeled dimers. A typical preparation starting with 90 μ L of 15 nM dimeric DNA nanotubes yields 600 μ L of \sim 1 nM purified SiR-labeled DNA nanotubes.

mEGFP-pAzF cloning

The sequence for mEGFP was cloned from plasmid pFA6a-mEGFP-kanMX6 (Addgene plasmid # 87023; RRID:Addgene_87023), and was inserted into destination vector pZE21-GFP-NHis-0TAG generated by the Isaacs lab⁵. First, overlap-extension PCR was used to add an EcoRI restriction site and a 6 \times His tag to the N-terminal of mEGFP, and a TAG codon and BamHI restriction site to the C-terminus. The resulting PCR product and destination vector were both digested with EcoRI and BamHI and purified by agarose gel electrophoresis. The gel-purified products were then ligated using T4 ligase. The final plasmid introduced into the GRO contained mEGFP with a 6 \times His N-term tag and a C-term TAG codon with inducible expression controlled by a pLtetO promoter. DH5 α cells were transformed with this plasmid and plated on kanamycin-selective agar plates. 20 colonies were picked and PCR tested with the forward and reverse primers used to clone the mEGFP insert. 4 colonies that produced the expected PCR result were grown overnight and extracted using a Miniprep kit (Qiagen). The resulting plasmid DNA was sequenced. Of the 4 sequenced colonies, 1 contained the exact 6 \times His-mEGFP-TAG sequence as designed. A small volume of the DH5 α culture with the correct mEGFP was stored at -80°C in 25% glycerol.

GRO transformation

Recoded *E. coli* Δ mutS:Zeo (Δ 1prfA):tolC^{5,6} was transformed with the plasmid 6 \times His_mEGFP-TAG (see above) and orthogonal translation system plasmid pAzFRS.1.t1⁵, both generated by the Isaacs lab, and plated on agar containing chloramphenicol and kanamycin. A resulting colony was picked and used to grow a \sim 5 mL culture, \sim 1 mL of which was stored at -80°C in 25% glycerol.

mEGFP-pAzF overexpression (adapted from ref 6)

A 100 mL 2 \times YT starter culture supplemented with chloramphenicol and kanamycin was inoculated with a miniscule volume from the glycerol stock of GRO cells transformed with 6 \times His_mEGFP-TAG and pAzFRS.1.t1 plasmids and grown at 34°C overnight. This starter culture was used to inoculate a 1L expression culture supplemented with chloramphenicol, kanamycin, pAzF, and arabinose. The expression culture was grown at 34°C to confluency (OD₆₀₀ = 0.5–0.8), and then mEGFP expression was induced with addition of anhydrotetracycline (aTc). The induced culture was grown for \sim 16 hours at 34°C. Then cells were pelleted by centrifugation at 4,000 \times g for 15 minutes. Supernatant was discarded and cell pellets were flash frozen and stored at -80°C.

mEGFP(pAzF) His-trap FPLC purification

Cell pellets were thawed on ice and resuspended in lysis/wash buffer (1 \times PBS pH 7.4 + 25 mM imidazole, supplemented with a protease inhibitor cocktail (Roche)). Resuspended cells were lysed using a homogenizer, lysate was centrifuged at 35,000 RPM for 45 minutes, and supernatant was collected and filtered using 0.45 μ m filters. A HisTrap column was conditioned with lysis/wash buffer, and then filtered lysate was circulated \sim 2.5 \times over column to bind. The column was then washed with \sim 3 column

volumes of lysis/wash buffer, which was collected. Bound protein was then eluted with elution buffer (1× PBS pH 7.4 + 500 mM imidazole), and fractions were collected. Fractions most likely to contain the desired product were selected by reviewing the FPLC traces (absorption at 254 & 280 nm) and were run in a reducing 12% Bis-Tris SDS-PAGE gel. Fractions confirmed to contain the desired products were pooled and buffer exchanged into lysis/wash buffer using Amicon 10k filters, then purified a second time using the HisTrap column. Fractions from the second HisTrap purification were run on a SDS-PAGE gel as before to identify the best fractions, which were then pooled, buffer exchanged into 1×PBS, pH 7.4, and measured for concentration using a BCA assay (Pierce). Finally, glycerol was added to the purified mEGFP(pAzF), which was then flash-frozen and stored at -80°C.

mEGFP – alkyne DNA conjugation and purification

Click reaction was adapted from protocols by Presolski et al.⁷ mEGFP(pAzF) was reacted with an excess of alkyne DNA (Table S1) for 1 hr at 30°C in degassed click reaction buffer (0.1 M potassium phosphate, 0.25 mM CuSO₄, 1.25 mM THPTA, 5 mM aminoguanidine HCl, 5 mM sodium ascorbate, pH 7). The reaction was then quenched by adding EDTA to a final concentration of 2.5 mM. Anion exchange was then performed using Pierce Strong Anion Exchange Spin Columns following the manufacturer's directions. Fractions were collected and stored O/N at 4°C before running on a 12% SDS-PAGE gel (Figure S6). Fractions confirmed to contain mEGFP-DNA conjugate but not the unreacted mEGFP were buffer exchanged into 1×PBS using 10k Amicon filters before size exclusion purification. Size exclusion was performed using a Superdex 75 Increase 10/300 column (Cytiva) connected to an ÄKTA FPLC system (Cytiva), and fractions were collected and stored at 4°C O/N before checking with SDS-PAGE (Figure S7&S8).

SiR-azide – alkyne-DNA click reaction

SiR-azide (Spirochrome) was reacted to alkyne DNA (Table S1) using the same protocol as mEGFP conjugation (above).

Urea-PAGE Purification of SiR-DNA conjugate.

SiR-DNA conjugate was mixed 1:1 with denaturing tracking dye buffer (90% formamide, 10 mM NaOH, 1 mM EDTA-Na₂, 0.1% xylene cyanole) and heated 10 minutes at 95°C. Sample was removed from heat and immediately chilled on ice before being loaded into a denaturing polyacrylamide gel (12% acrylamide, 8.3 M urea, 89 mM tris base, 89 mM boric acid, 2 mM EDTA pH 8.0). Each gel well was loaded with 20 µL of SiR-DNA conjugate at ~2 OD, and the loaded urea-PAGE gel was run in 1× TBE buffer (89 mM tris base, 89 mM boric acid, 2 mM EDTA, pH 8.0) for 2 hours at a constant current of 30 mA and at 37°C. The gel was removed from the running apparatus, wrapped in plastic, and visually inspected on a transilluminator under white light and 302 nm UV to locate the migrated SiR-DNA conjugate. The desired SiR-DNA oligonucleotide was observable as a blue band under white light and as dark shadow cast against a phosphor screen under 302 nm UV. The desired DNA band was excised with a clean razorblade. The gel fragments containing the SiR-DNA were diced into smaller pieces and placed into Freeze 'N Squeeze filters (Bio-Rad) along with 500 µL of elution buffer (500 mM

NH₄AC, 10 mM Mg(AC)₂•(H₂O)₄, 2 mM EDTA, pH 8.0). Freeze 'N Squeeze filters containing cut gel and elution buffer were wrapped in Al foil and agitated at room temperature for 8 hours. Filters were spun at room temperature at 8,000 rpm for 6 minutes to separate eluted SiR-DNA conjugate and gel. Eluted SiR-DNA was subsequently purified of organic contaminants via extraction with butanol (using a butanol:DNA volume ratio of 2:1). The extracted aqueous layer containing the SiR-DNA was then subjected to ethanol purification: 100% ethanol was added to the SiR-DNA solution at a 2:1 (v/v) ratio, mixed thoroughly, and then chilled at -20°C for 30 minutes. The tubes were then centrifuged at 13,000 rpm for 30 minutes at 4°C to pellet the SiR-DNA. The supernatant was decanted, and the SiR-DNA pellets were washed with ice-cold 70% ethanol followed by another 13,000-rpm spin for 10 minutes. After decanting the supernatant, the SiR-DNA pellets were air-dried overnight at room temperature in dark. After drying, solid SiR-DNA pellets were either dissolved in water/buffer of choice or stored dry at -20°C. Purification of the desired SiR-DNA fragment was confirmed by subsequent urea-PAGE analysis and comparison with Ultra Low Range DNA Ladder (Invitrogen). Importantly, the² entire purification protocol was performed in dim lighting conditions with foil coverings over tubes and the gel running apparatus to minimize potential photobleaching of the SiR-DNA conjugate.

Generation of *B. subtilis* cells expressing dnaC-mEGFP

B. subtilis PY79 cells expressing dnaC-mEGFP (strain NW001) was constructed using plasmid DNA and a 1-step competence method. Original plasmid (dnaC-GFPmut2) was obtained from Alan D. Grossman at MIT Department of Biology and mutated to mEGFP using QuikChange Lightning kit (Agilent) following manufacturer's instructions. Mutations were confirmed by sequencing.

Imaging of mEGFP standards and *B. subtilis* cells

mEGFP-labeled DNA nanotubes were immobilized on a coverslip as previously described⁸ for quality control imaging (not shown), and on a 2% agarose pad made with 1× M9 salts medium (Gibco) and equilibrated in arabinose minimal medium (1x Spitzizen's salts (3 mM (NH₄)₂SO₄, 17 mM K₂HPO₄, 8 mM KH₂PO₄, 1.2 mM Na₃C₆H₅O₇, 0.16 mM MgSO₄•(7H₂O), pH 7.0), 1x metals (2 mM MgCl₂, 0.7 mM CaCl₂, 0.05 mM MnCl₂, 1 μM ZnCl₂, 5 μM FeCl₂, 1 μg/ml thymine-HCl), 1% arabinose, 0.1% glutamic acid, 0.04 mg/ml phenylalanine, 0.04 mg/ml tryptophan, and as needed 0.12 mg/ml tryptophan) for generating calibration curves (Figure 1c & S12). Cells were prepared as previously described by Mangiameli et al.⁹ with slight modifications. Briefly, *B. Subtilis* (strain NW001) were cultured overnight in arabinose minimal medium in a shaking incubator at 30°C. Overnight cultures at an OD₆₀₀ of 0.4–0.9 were diluted back to an OD₆₀₀ of 0.2 and incubated again for about 2 hr until they reached approximately OD₆₀₀ 0.4. Cells were mounted on a 2% agarose pad, which was made with 1× M9 salts medium (Gibco) and equilibrated in arabinose minimal medium, using a gene frame (Bio-Rad). Note that both cells and the mEGFP standards were re-suspended in the arabinose minimal medium containing >2 mM Mg²⁺. We found no evidence of degradation or loss of fluorescence when standards were incubated in imaging media containing as low as 1 mM MgCl₂ (Figure S25). Fluorescence microscopy was performed using a Leica DMI8 Wide-field Inverted Microscope equipped with an HC PL

APO 100×DIC objective, an iXon Ultra 888 EMCCD Camera (Andor Technology) and Lumencor's Spectra-X LED Light Engine as the source of light. Excitation light transmission was set to 50% and exposure time for GFP ($\lambda_{EX}=470/40$; $\lambda_{EM}=525/50$) was 1 sec. See Table S4 for more details. Cells were concentrated 10× by centrifugation (3300×g for 30 sec) prior to visualization. Cells were imaged at RT. Images were acquired with Leica Application Suite X, and analysis and processing were performed using the ImageJ software.

Image processing of wide-field microscopy images

Background fluorescence from agar pads and cell autofluorescence was estimated by measuring line profiles spanning cells and origami, then subtracted from the image. Spots were picked using MicrobeJ¹⁰, and were subsequently selected manually: DNA-origami spots in the mEGFP channel were selected if they were non-overlapping and colocalized with signal in the Alexa Fluor 647 channel; dnaC spots were selected if they were clear, round puncta within cell boundaries (2 out of 77 puncta were excluded because of their abnormally large size and intensity). These intensities were plotted as a histogram and fit to a sum of two Gaussians function using GraphPad Prism¹¹. The workflow is summarized in Figure S14.

CLC (Clathrin Light Chain)-HaloTag CRISPR/Cas9 gene editing

CLC-HaloTag CRISPR cells were generated by transfecting a repair template that has Halo tag and the gRNA specific to the targeted gene. The following gRNA sequence was used for the CLC genomic DNA (Gene ID 1211): 5'- GCAGATGTAGTGTTCACACA GGG-3' (PAM sequence is underlined). This gRNA was cloned into the SpCas9 pX330 plasmid (Addgene plasmid #42230)¹² by BbSI site. The homologous repair plasmid with HaloTag was constructed by pEGFP-C1 plasmid. The right homology arm (~1 kb) was cloned into pEGFP-C1 using EcoO109I site. The left homology arm (~1 kb) was cloned with PCR fragment of HaloTag by In-Fusion HD Cloning kit (Takara Bio USA, Inc.) using AseI and BamHI cutting sites. The target sequence (PAM site) was mutagenized in the right homologous arm.

The pX330 plasmid with gRNA of CLC and the homologous repair plasmid were transfected in HeLa CCL-2 cells using Lipofectamine 3000 (Thermo Fisher). After 48hrs post-transfection, cells were selected by G418. After selection, cells were screened by single cell cloning with serial dilution protocol in 96 well plate and immunoblot.

CLC-Halo cell cultures

*Halo-CLC*¹³ CRISPR/Cas9 HeLa cells were cultured in Dulbecco's modified Eagle medium (DMEM) (Gibco, 21063-029) supplemented with 10% FBS. All cells were cultured at 37°C in 5% CO₂ incubator.

CLC-Halo labeling with SiR-chloroalkane (SiR-CA) in HeLa cells

Cells were seeded on 35 mm glass bottom dishes (Mattek P35G-1.5-14-C) 24 hrs before imaging. On the day of imaging *Halo-CLC* expressed in cells were labelled with 5 μ M near far-red silicon rhodamine (SiR): SiR-chloroalkane (a gift from Promega) for 30 min at 37°C. Subsequently the cells were washed three times and placed back in 37°C incubator for 1 hr.

Imaging SiR standards and SiR labeled CLC-Halo in HeLa cells

SiR-labeled DNA nanotube dimers were immobilized on a Mattek dish as previously described⁸, in Live Cell Imaging Solution (LCIS) (Thermo Fisher, pH 7.4, A14291DJ). We found no evidence of degradation or loss of fluorescence when standards were incubated in imaging media containing as low as 1 mM MgCl₂ (Figure S25). The cells were imaged live in LCIS on TiE inverted Nikon spinning disc confocal microscope, using a 60×/1.4 Oil objective. SiR labels were imaged using a 647 nm laser line (190 mW, measured at the fiber tip) using Nikon's Perfect Focus System. See Table S4 for more details. Laser power was maintained constant throughout the imaging session after adjusting to avoid saturation. Several images of glass bottom dishes without cells were also captured at the same focal point for background correction post acquisition (see below).

Image processing of confocal micrographs

First, background from media and the cell dish was approximated by averaging 10 images of empty dishes to generate a new image. This image was then subtracted from all images containing DNA-origami nanotubes or HeLa cells. SiR puncta in DNA-origami images were picked using a custom TrackMate script (Do_subpixel_localization: True, Radius: 0.8, Threshold: 6.0, and Do_median_filtering: False), and used to construct the calibration curve (Figure 2d). A background-subtracted image of cells was median filtered (20 px radius) to generate the approximate background intensity from cell autofluorescence and nonspecific SiR-CA labeling. This image was then subtracted from the image of cells. CLC-SiR spots in cells were then picked manually by size and morphology. Only spots that were well-defined, nonoverlapping, in-focus, and circular, were selected. These criteria were selected based on the morphological differences between coated pits and plaques previously described.¹⁴ CLC-SiR intensities were then converted to molecule number using the calibration curve. The workflow is summarized in Figure S24.

Supplementary Figures

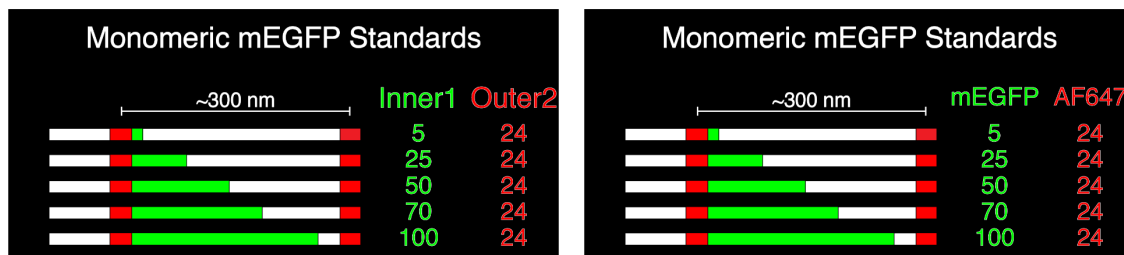


Figure S1. Diagrams of mEGFP standards. Left: number and names of handle sequences. Right: number and names of fluorophores.

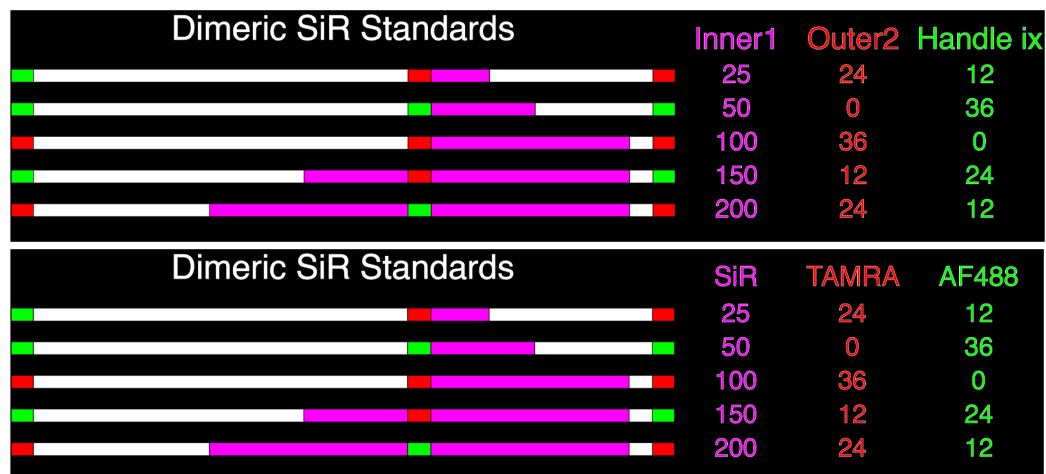
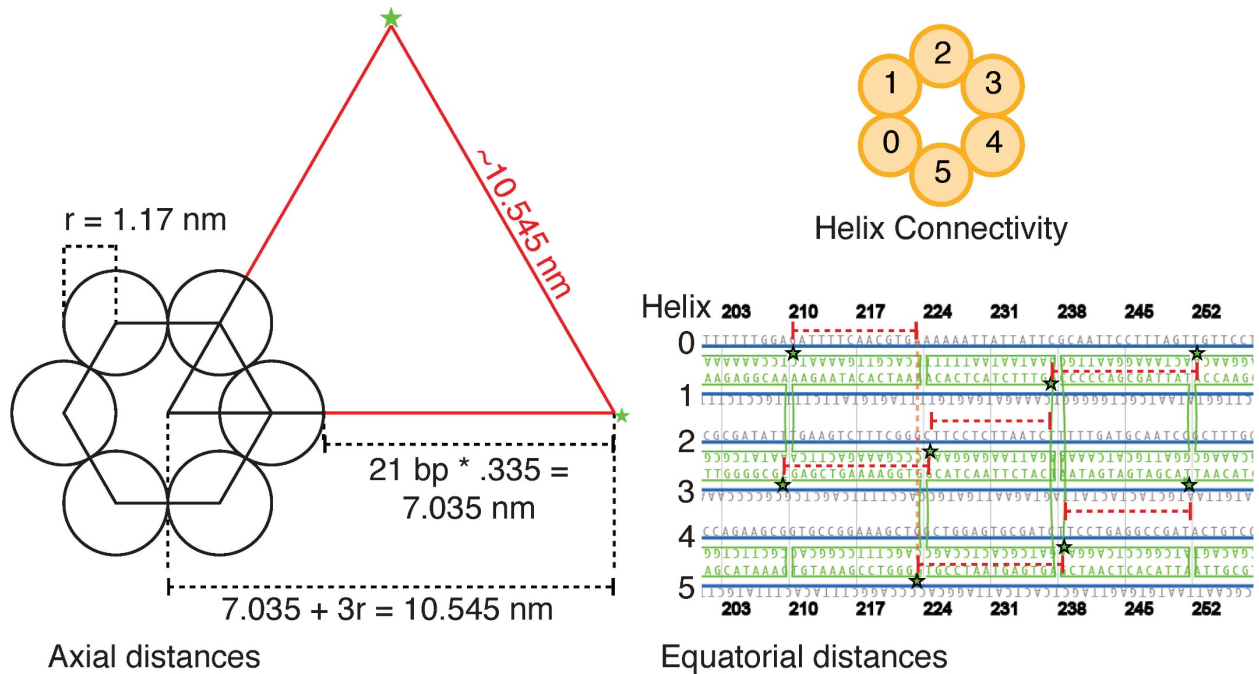


Figure S2. Diagrams of SiR standards. Top: number and names of handle sequences. Bottom: number and names of fluorophores.



Helix A	Helix B	Axial D (nm)	Equatorial D (NT)	D/NT (nm)	Equatorial D (nm)	Total D (nm)
0	1	10.545	16	0.335	5.36	11.83
1	2	10.545	14	0.335	4.69	11.54
2	3	10.545	16	0.335	5.36	11.83
3	4	10.545	14	0.335	4.69	11.54
4	5	10.545	16	0.335	5.36	11.83
5	0	10.545	14	0.335	4.69	11.54

Figure S3. Distances between fluorophores. 21-bp handles extend from the 3' end of green staple strands (green stars). Distances between adjacent fluorophores were calculated as follows: $\sqrt{(\text{axial } d)^2 + (\text{equatorial } d)^2}$. The radius of a double helix in a 6hb nanotube was measured previously.¹⁵

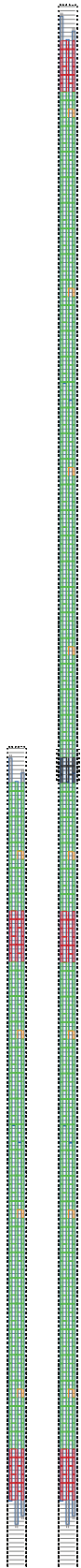


Figure S4. Design (caDNAno¹) diagrams of DNA-origami nanotubes

Staples in monomeric (left) and dimeric (right) structures are color-coded. All handles extend from 3' end.

Gray: poly-T end caps.

Red: Handles reserved for barcoding fluorophores. Handles are outer 2 or handle ix, depending on structure.

Green: optional attachment of inner 1 handle (for mEGFP/SiR).

Orange: non ATG 1 handle for biotin.

Black: linker DNA for dimerization.

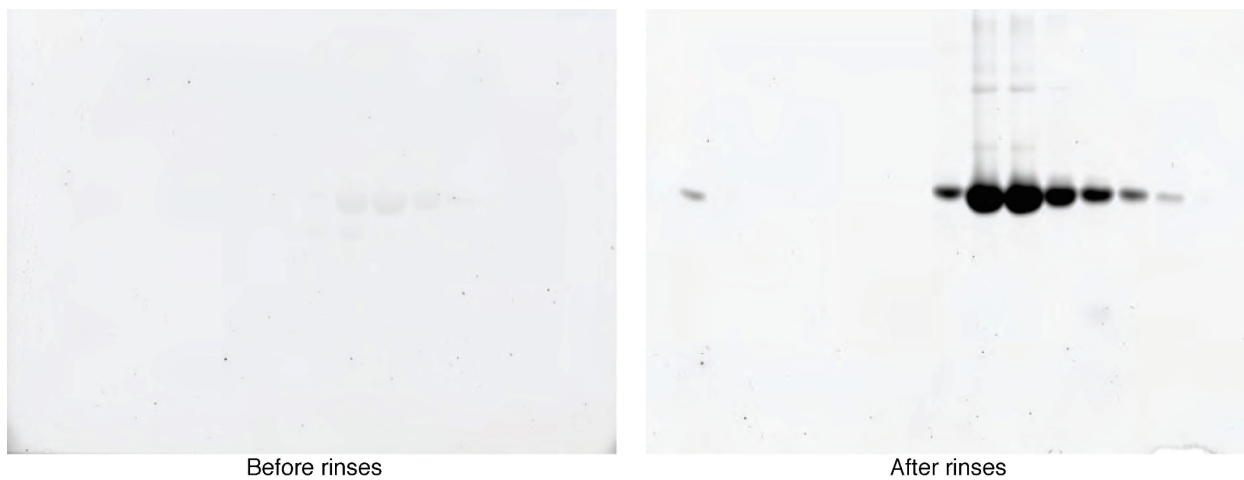


Figure S5. mEGFP in-gel fluorescence recovery. After rinsing in water 3× 20 min, enough fluorescence was recovered to allow gel imaging in the 488 channel.

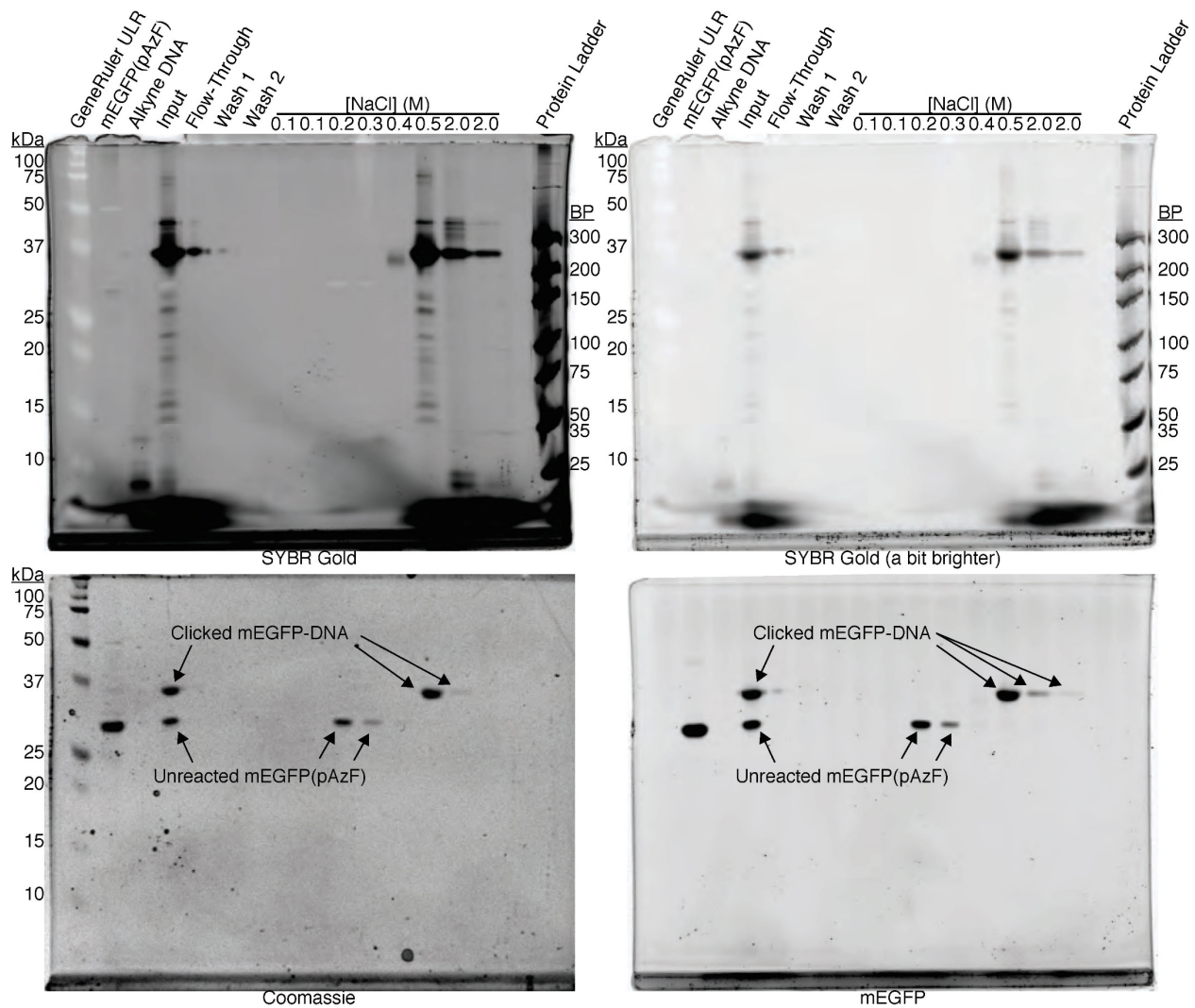


Figure S6. mEGFP-DNA conjugates after anion-exchange purification. The expected ~7 kDa shift in reacted mEGFP:anti-inner1 is clearly visible when comparing unreacted mEGFP(pAzF) and the Input reaction mixture. Unreacted mEGFP(pAzF) began to elute at an ionic strength of 0.2 M NaCl, while mEGFP:anti-Inner1 eluted above 0.4 M NaCl. Incomplete reaction of mEGFP(pAzF) is possibly due to imperfect incorporation of pAzF at the C-term and azide reduction *in vivo*.¹⁶

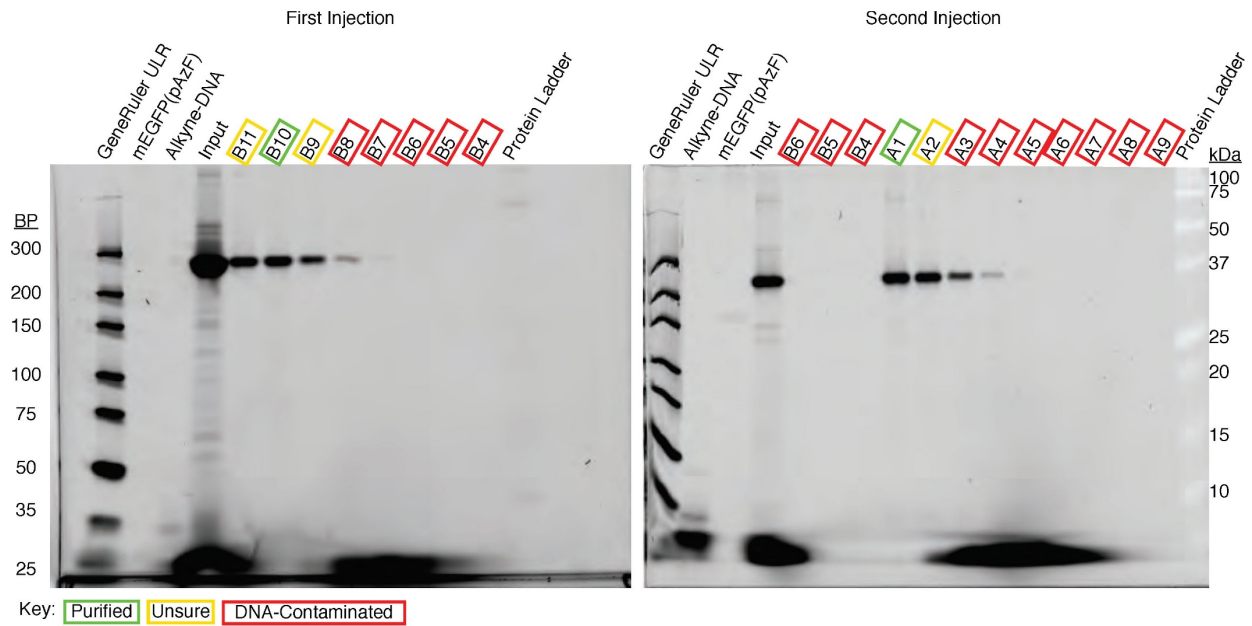


Figure S7. mEGFP-DNA conjugates after size-exclusion purification. Anion-exchanged reaction mixtures were purified (two rounds) by size-exclusion chromatography to remove unreacted alkyne-DNA. Gels were stained by Sybr Gold and imaged in the corresponding channel.

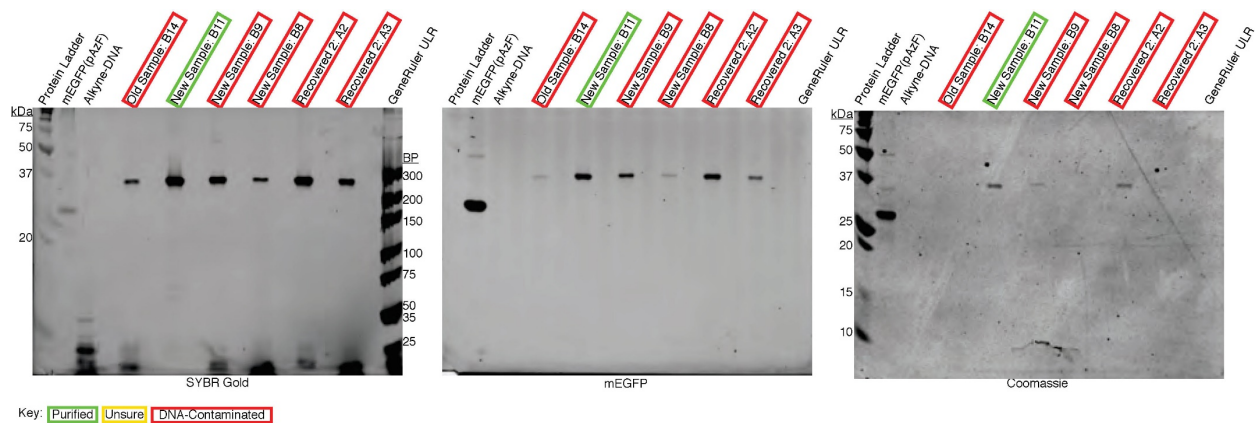


Figure S8. Purified mEGFP-DNA conjugates. Neither unreacted mEGFP nor DNA were found in purified fractions (B11).

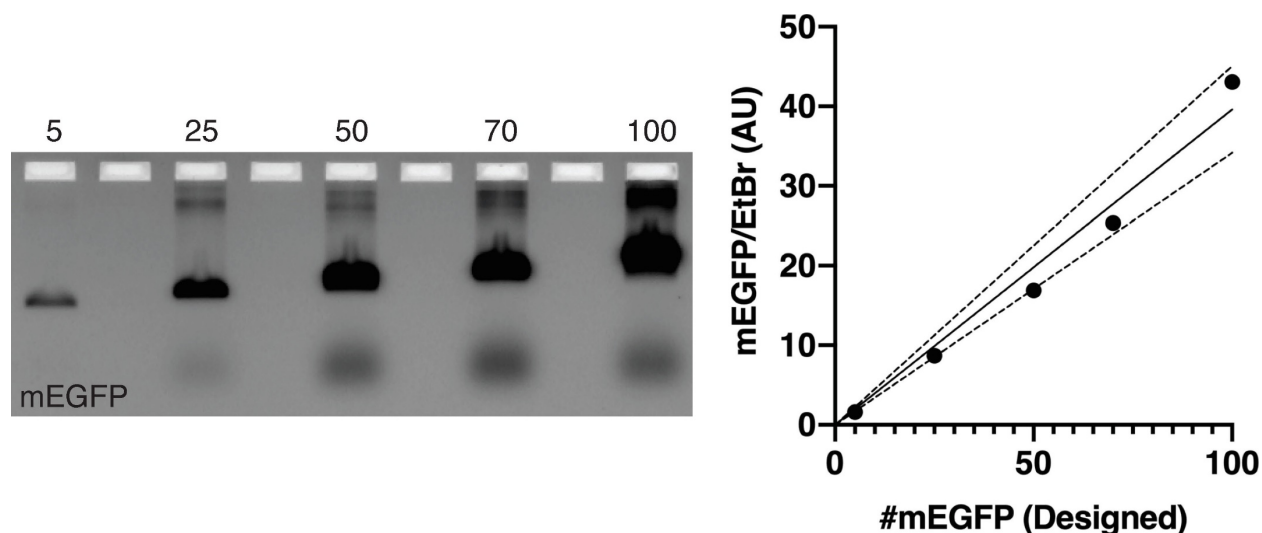


Figure S9. mEGFP standards electrophoresed in an agarose gel. DNA nanotubes designed to accommodate 5–100 mEGFP were labeled with mEGFP-antihandles and run in a non-denaturing agarose gel (left). After the mEGFP channel (488 nm) was imaged, the gel was stained with 0.5 $\mu\text{g}/\text{mL}$ EtBr and imaged again (532 nm). The band intensities were quantified using ImageQuant TL, and normalized mEGFP fluorescence was plotted (right). A standard linear regression¹¹ yielded a slope of 0.3962 (solid line) with a 95% confidence interval (CI) of 0.3417 to 0.4508 (dashed lines).

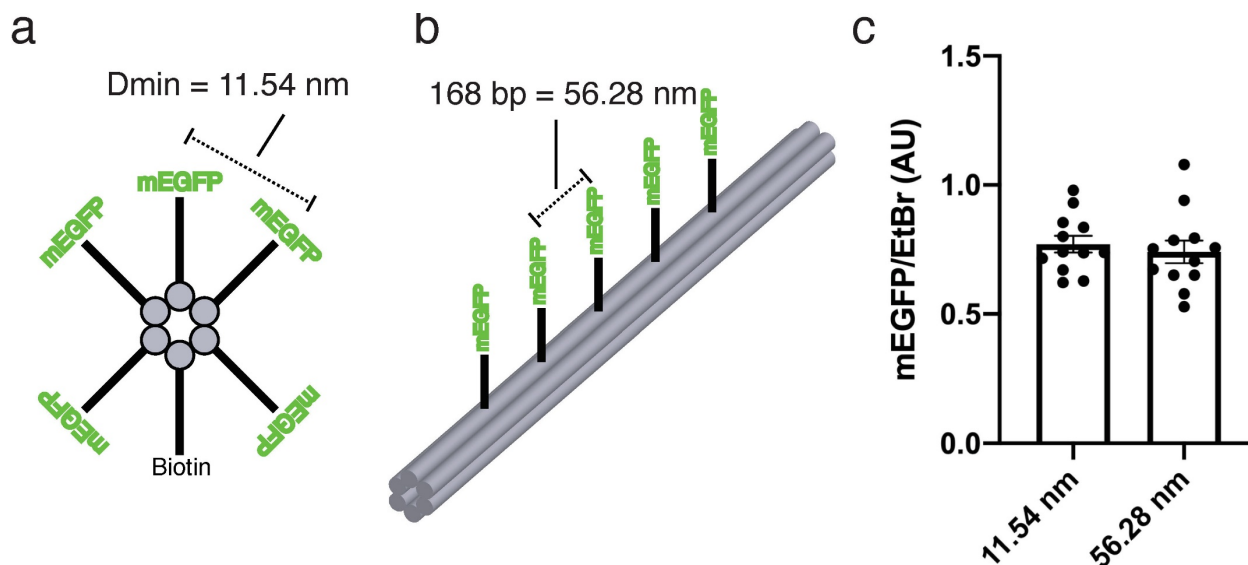


Figure S10. Test for mEGFP self-quenching. 6 Structures were designed to host 5 \times mEGFPs, 3 with the same inter-protein distances as the rest of this work (a), and 3 had mEGFP placed every ~ 56 nm (b). In each structure, unique handle locations were chosen to negate the influence of specific handle incorporation efficiencies. All 6 structures were run in quadruplicate in a non-denaturing agarose gel, and imaged before and after EtBr staining. Normalized mEGFP band intensities were nearly identical, regardless of spacing (mean \pm SEM), showing no sign of self-quenching.

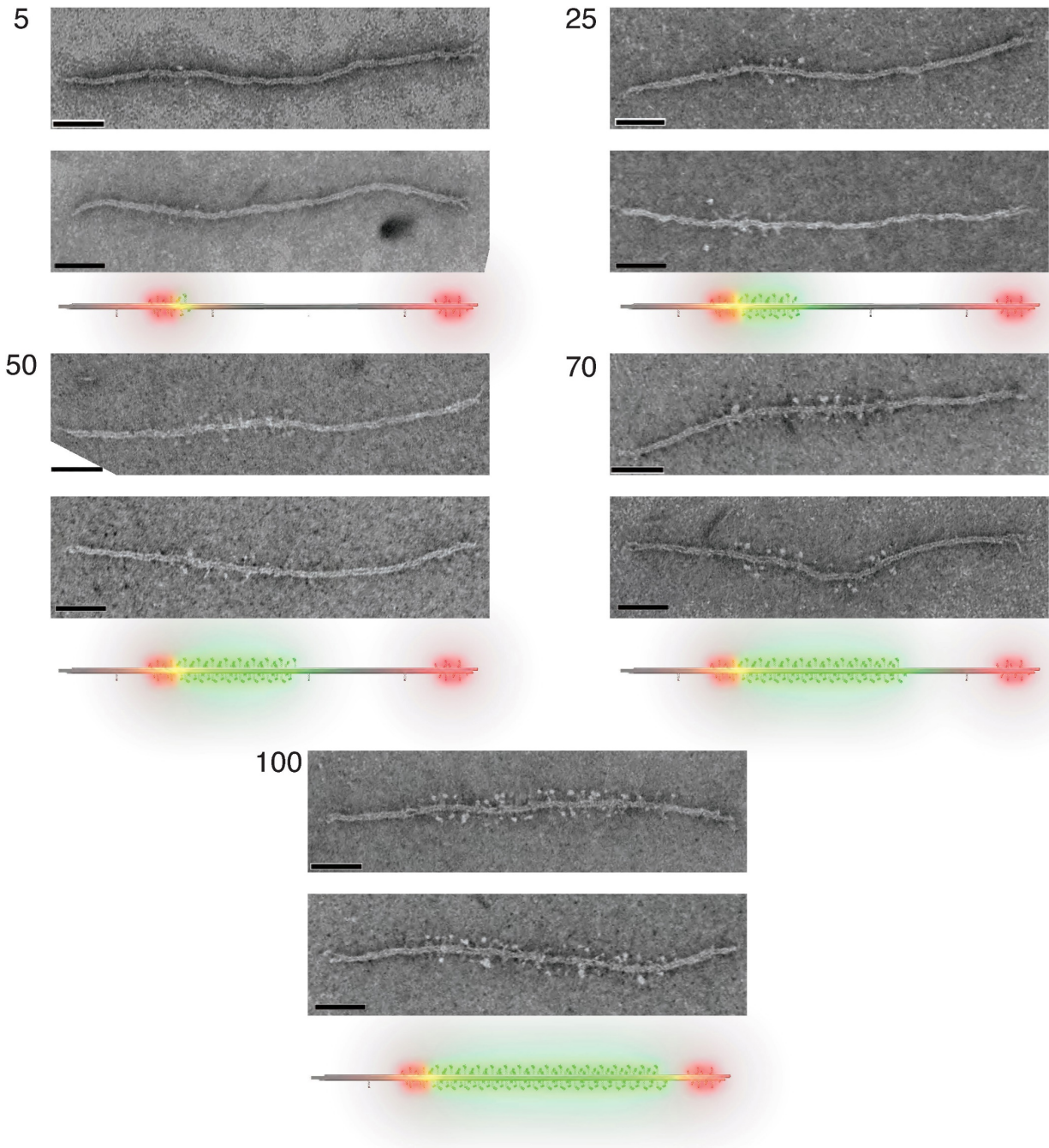


Figure S11. TEM micrographs of mEGFP standards. 5, 25, 50, 70, & 100 indicate the number of mEGFP each structure is designed to accommodate. All structures have 12 Alexa Fluor 647 at each end. Due to the resolution limit of negative-stain TEM, we do not expect to resolve every single mEGFP molecule. Nevertheless, in selected images, small dots (mEGFP) were found spanning the structures in the expected regions. Cartoon models were placed below micrographs (Green: GFP, Red: Alex Fluor 647) for direct comparison. Scale bars: 50 nm.

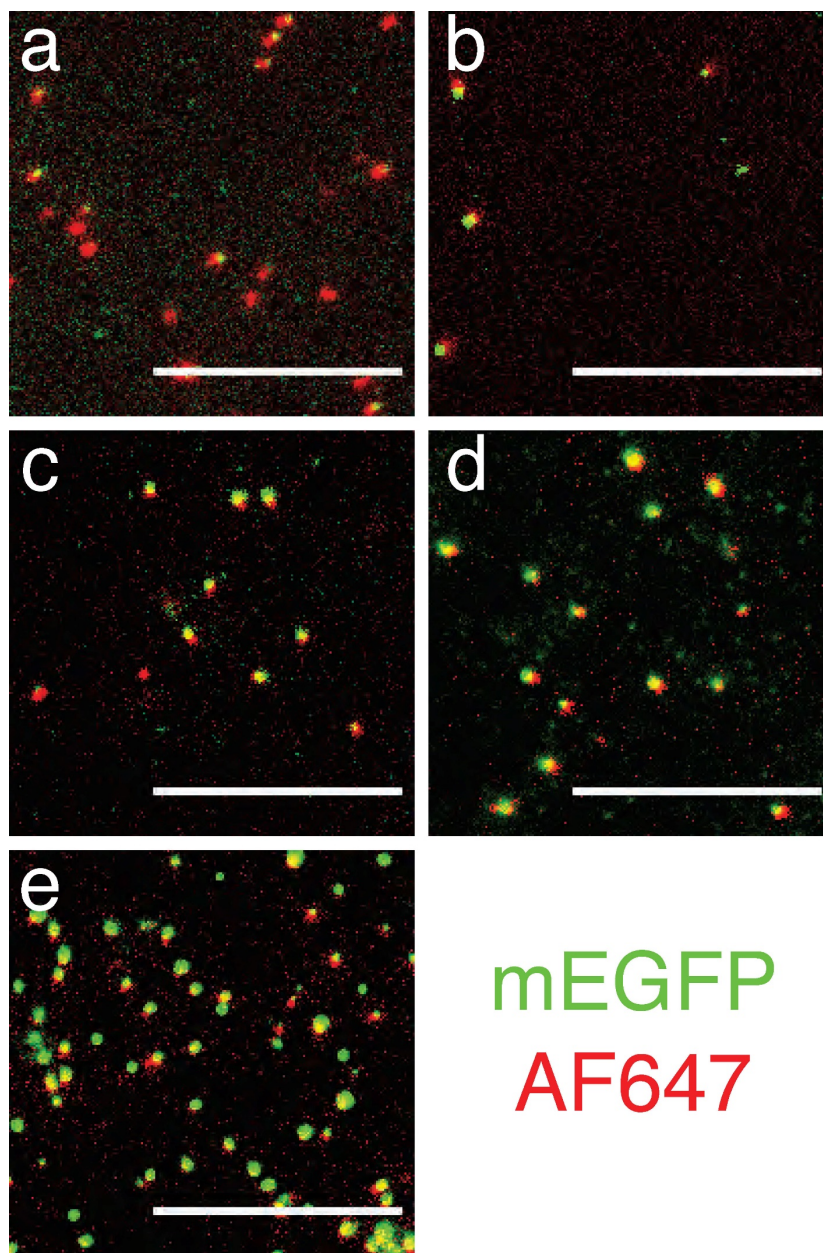


Figure S12. Wide-field fluorescence micrographs of mEGFP standards.. (a) 5 \times , (b) 25 \times , (c) 50 \times , (d) 70 \times , (e) 100 \times . All structures have 12 Alexa Fluor 647 at each end. Brightness and contrast for each image adjusted individually for clarity. Scale bars: 10 μm .

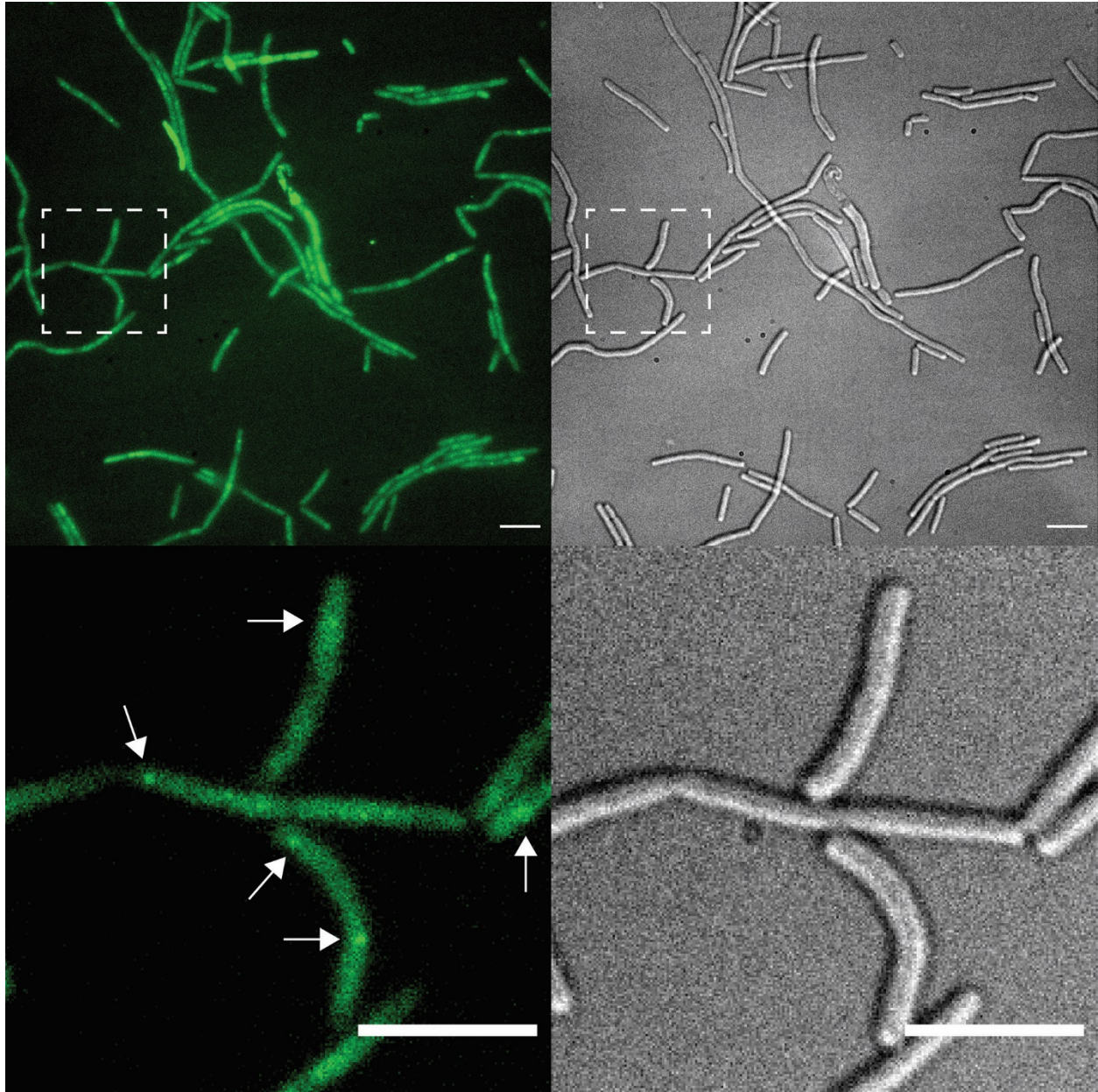


Figure S13. Wide-field fluorescence micrographs of *B. subtilis*. Representative image of *B. subtilis* (strain NW001) cells expressing dnaC-mEGFP (puncta indicated by arrows). Left: mEGFP (488 nm); right: differential interference contrast. Images in the bottom row are magnified from areas within dotted rectangles. Brightness and contrast for each image adjusted individually for clarity. Unlike Figure 1d, the fluorescence brightness is rescaled not to highlight individual punctum, but to show the overall cell shapes. Scale bars: 10 μm .

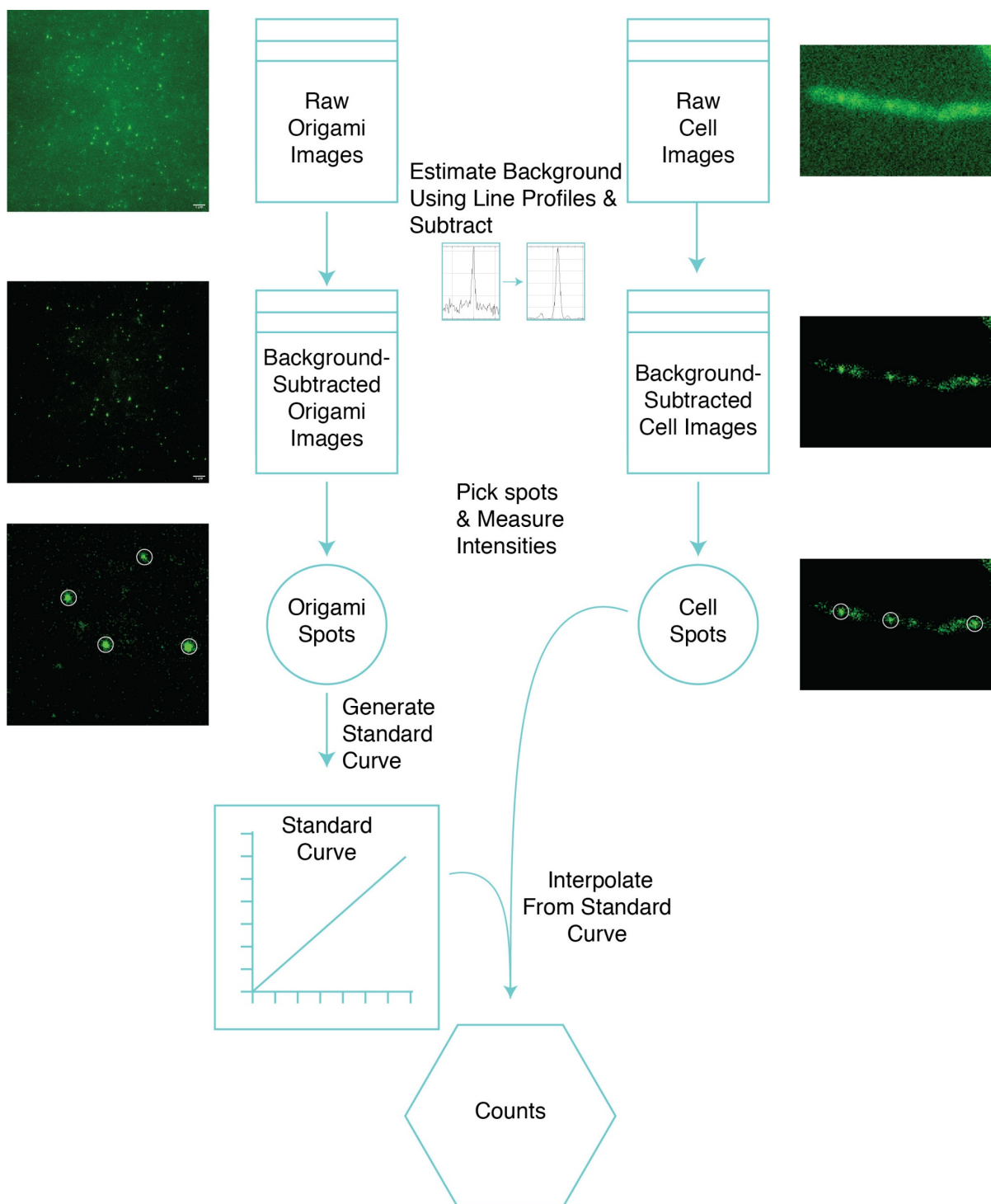


Figure S14. Image processing pipeline for mEGFP labeling. Background fluorescence from agar pads and cell auto-fluorescence was estimated by measuring line profiles spanning cells and DNA-origami standards, then subtracted from the image. Spots were picked using MicrobeJ¹⁰, and were subsequently selected manually (see Materials and Methods for criteria). These intensities were fit to a sum of two Gaussians function using GraphPad Prism¹¹.

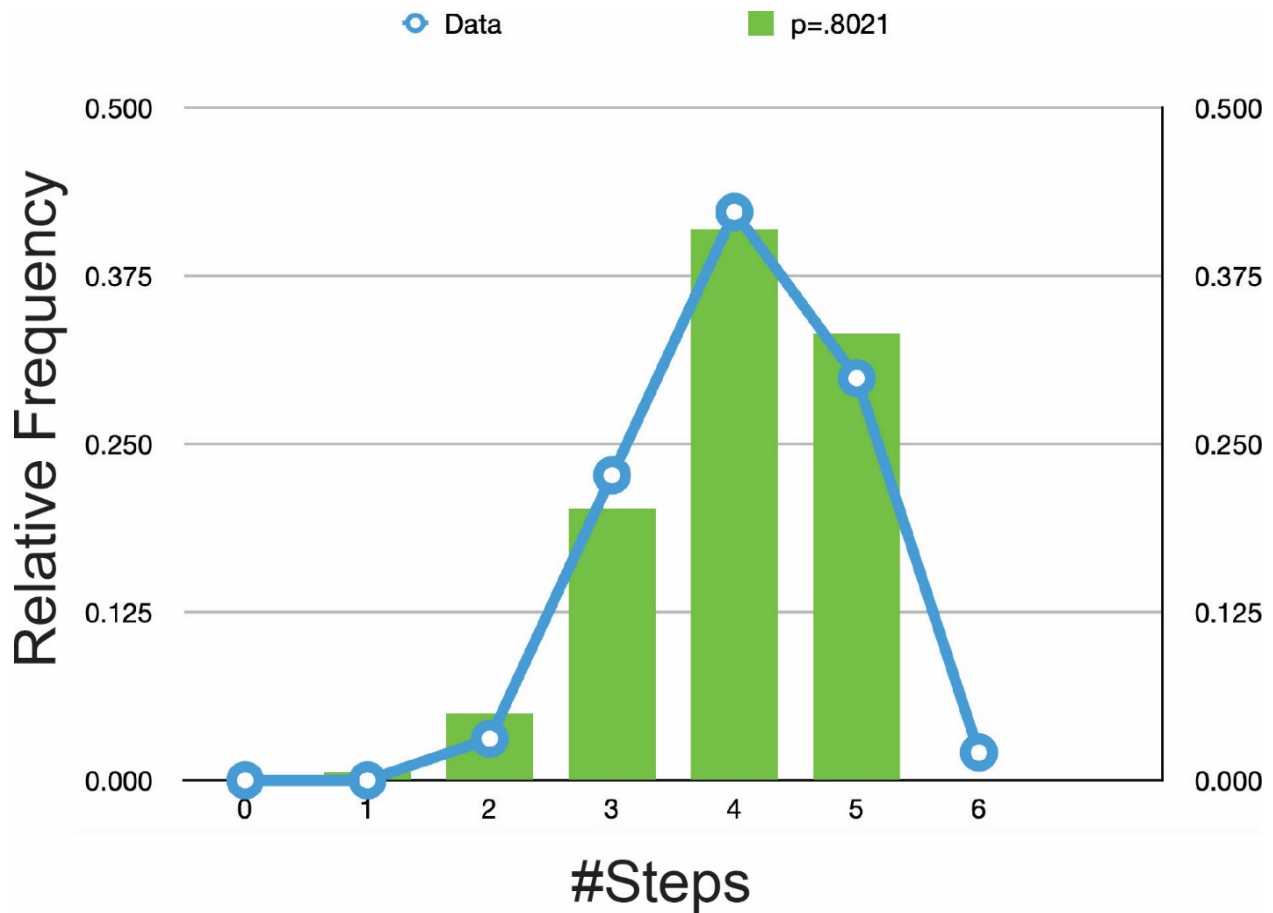


Figure S15. Handle occupancy estimation. Structures designed to host 5× mEGFP were labeled with Alexa Fluor 488-labeled antihandles and imaged on a Nikon TIRF microscope until fully bleached. The total photobleaching steps of the fluorescence traces were fit to a binomial function with MATLAB¹⁷. The best fit probability was $p=0.8021$, 95% CI = [0.7634 0.8370]. Note: 2 out of 97 traces showed 6 apparent steps, and were excluded from the binomial fit.



Figure S16. SiR-DNA conjugate analyzed by PAGE. SYBR Gold-stained 15% urea-PAGE gel of the SiR conjugate before (B) and after (A) purification. Ladder (L) is NEB Ultra Low Range DNA Ladder.

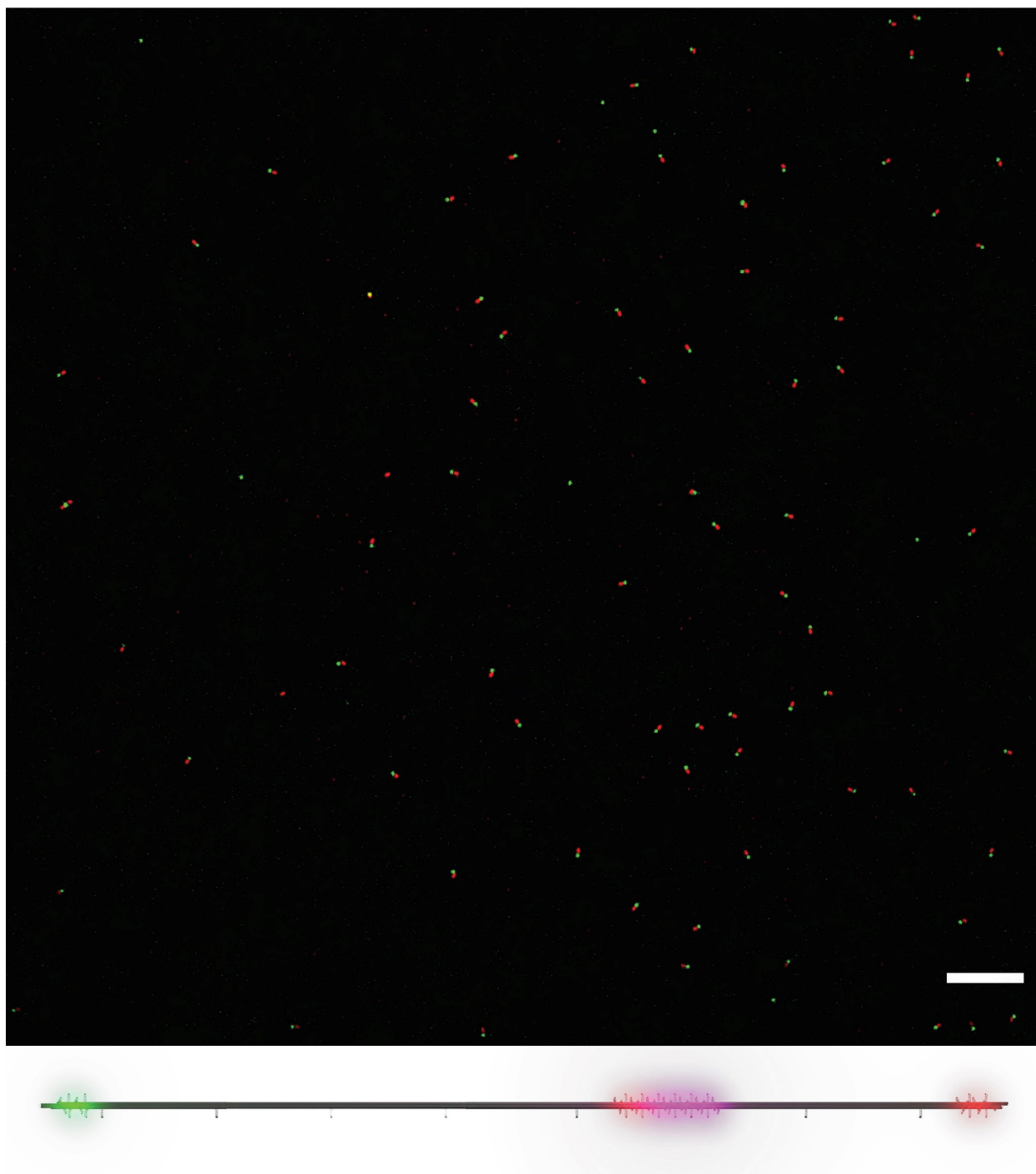


Figure S17. Fluorescent barcode pattern on 25× SiR standard. Top: confocal fluorescence micrograph showing the barcoding channels of Alexa Fluor 488 (green), and TAMRA (red). Scale bar: 10 μm . Bottom: A 3D model showing positions of barcoding fluorophores on the 25×SiR-labeled DNA-origami 6hb structure.

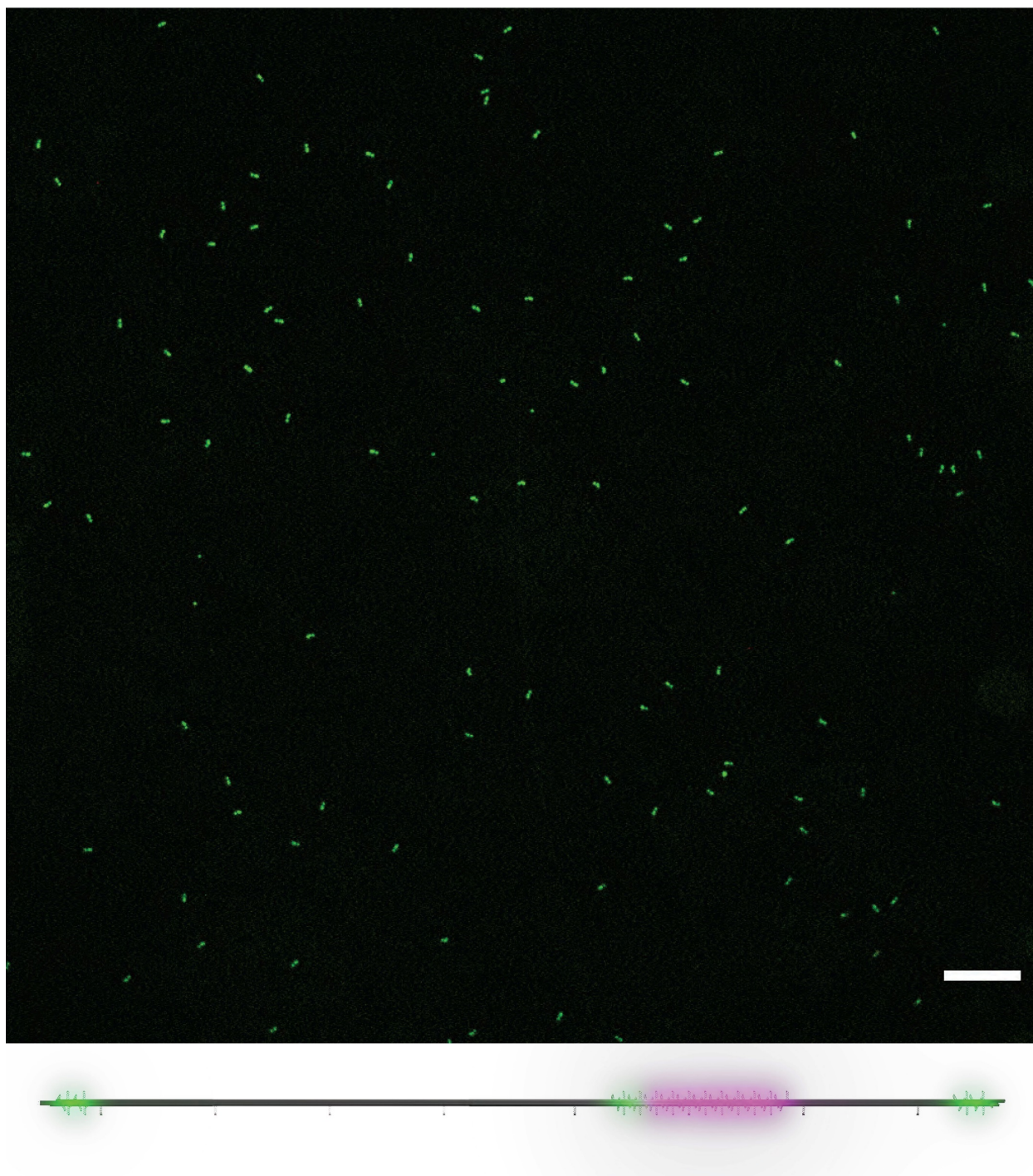


Figure S18. Fluorescent barcode pattern on 50× SiR standard. Top: confocal fluorescence micrograph showing the barcoding channel of Alexa Fluor 488 (green). Scale bar: 10 μm . Bottom: A 3D model showing positions of barcoding fluorophores on the 50×SiR-labeled DNA-origami 6hb structure.

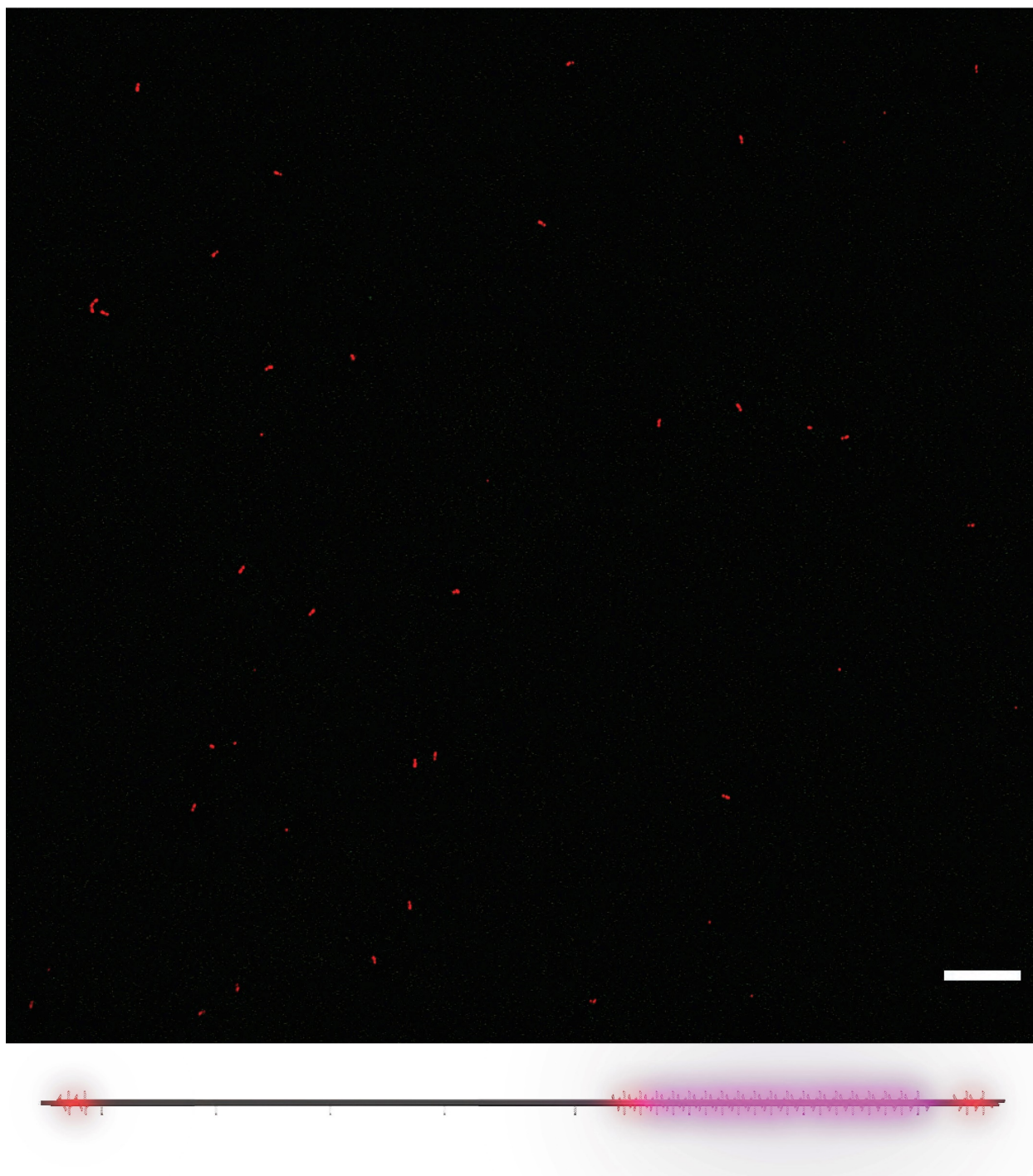


Figure S19. Fluorescent barcode pattern on 100× SiR standard. Top: confocal fluorescence micrograph showing the barcoding channel of TAMRA (red). Scale bar: 10 μm . Bottom: A 3D model showing positions of barcoding fluorophores on the 100×SiR-labeled DNA-origami 6hb structure.

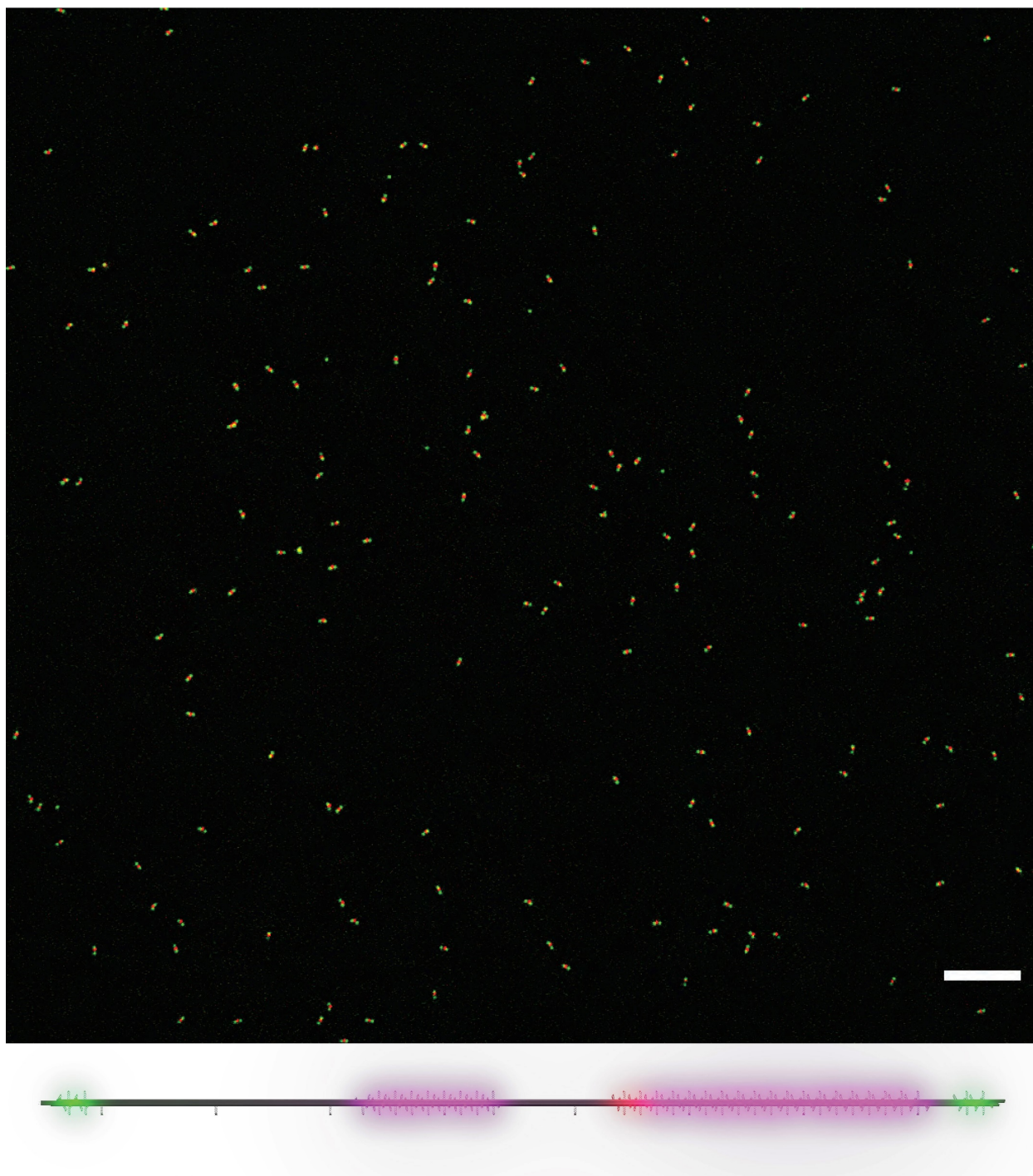


Figure S20. Fluorescent barcode pattern on 150× SiR standard. Top: confocal fluorescence micrograph showing the barcoding channels of Alexa Fluor 488 (green), and TAMRA (red). Scale bar: 10 μm . Bottom: A 3D model showing positions of barcoding fluorophores on the 150×SiR-labeled DNA-origami 6hb structure.

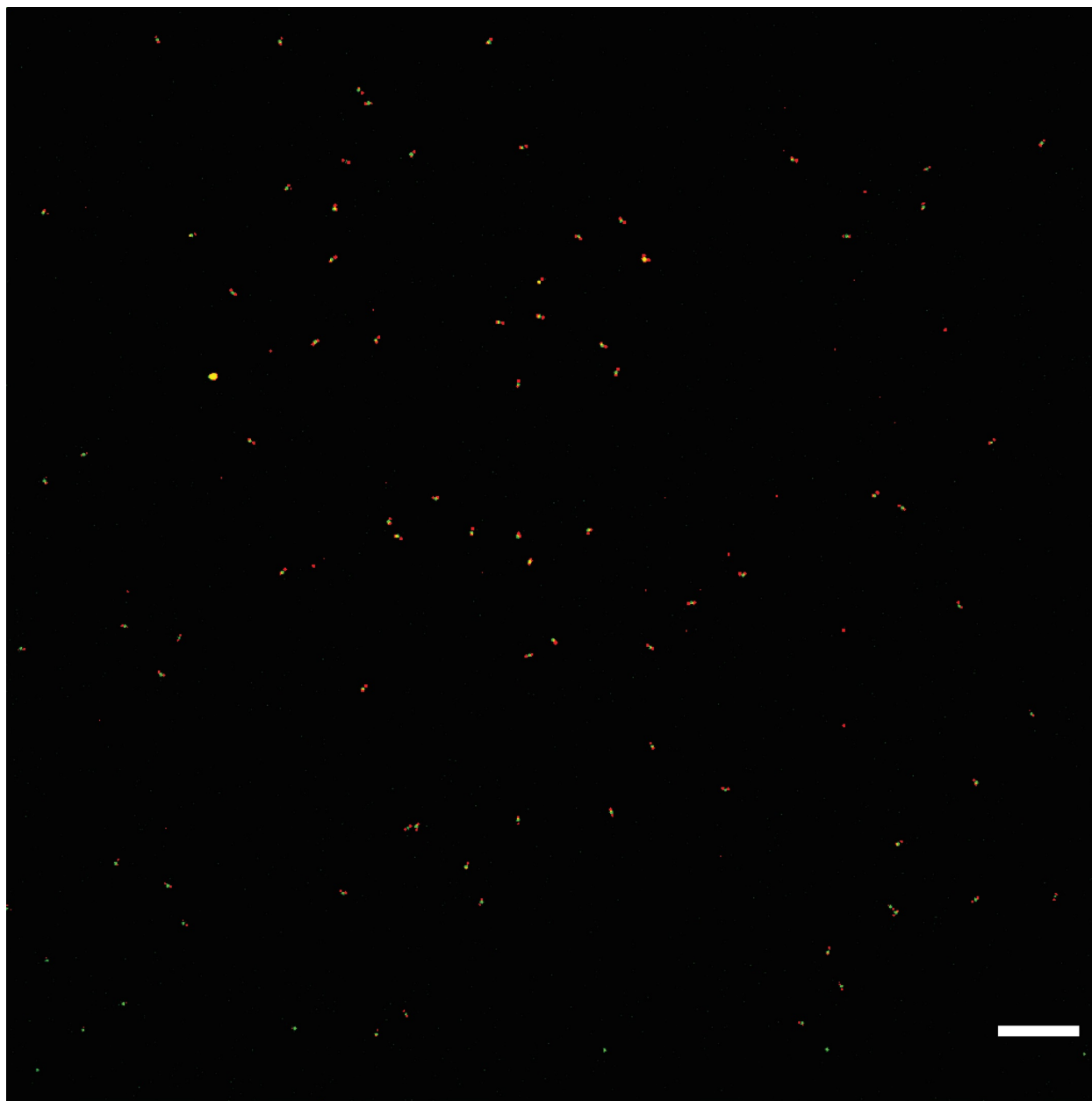


Figure S21. Fluorescent barcode pattern on 200× SiR standard. Top: confocal fluorescence micrograph showing the barcoding channels of Alexa Fluor 488 (green), and TAMRA (red). Scale bar: 10 μm . Bottom: A 3D model showing positions of barcoding fluorophores on the 200×SiR-labeled DNA-origami 6hb structure.

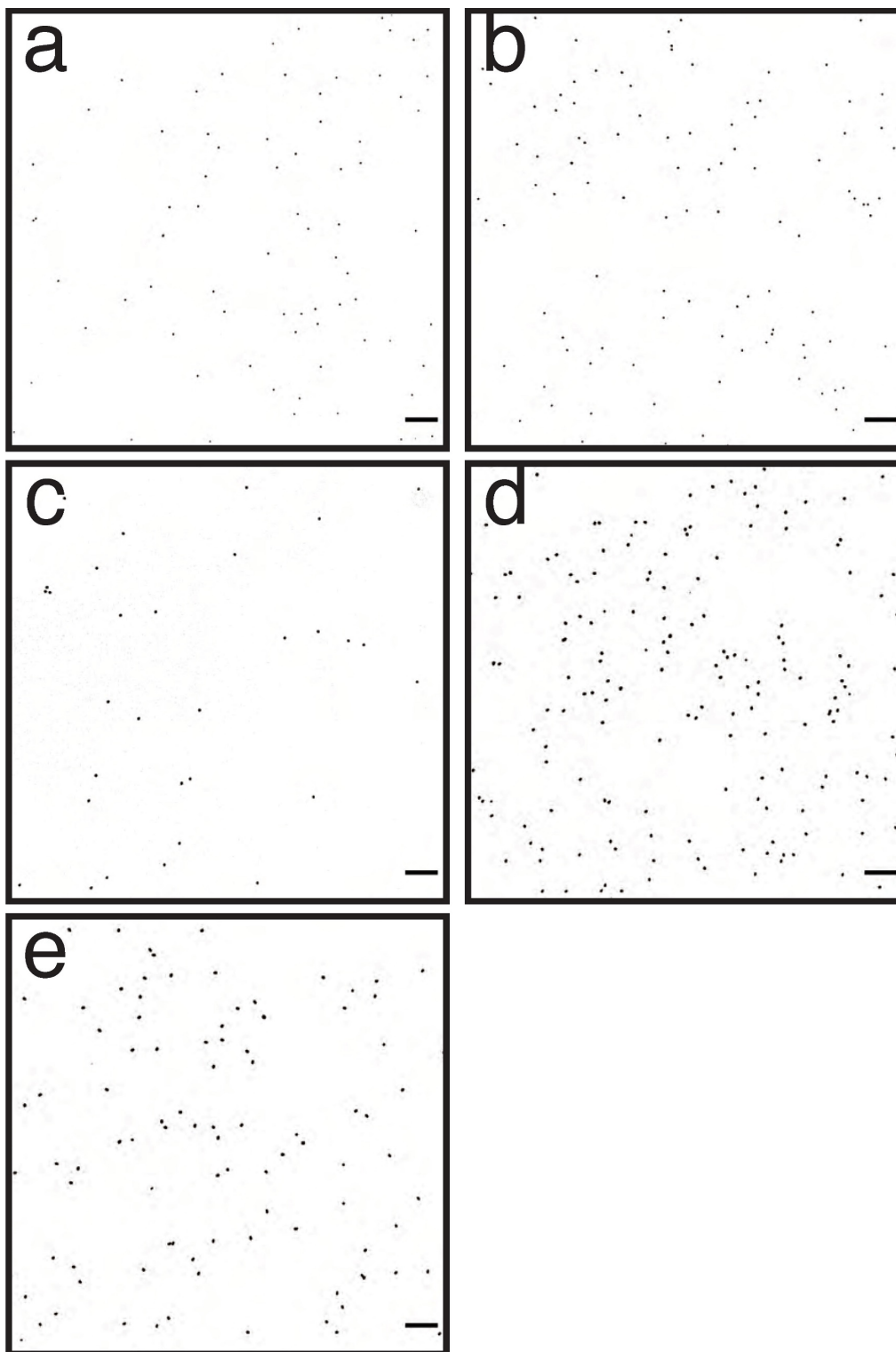


Figure S22. Confocal fluorescence micrographs of SiR standards. Panels show the SiR channel of Figure S17–S21, respectively: (a) 25× SiR, (b) 50× SiR, (c) 100× SiR, (d) 150× SiR, (e) 200× SiR. All panels are adjusted to the same brightness and contrast levels, and color-inverted for visual clarity. Scale bars: 10 μm .

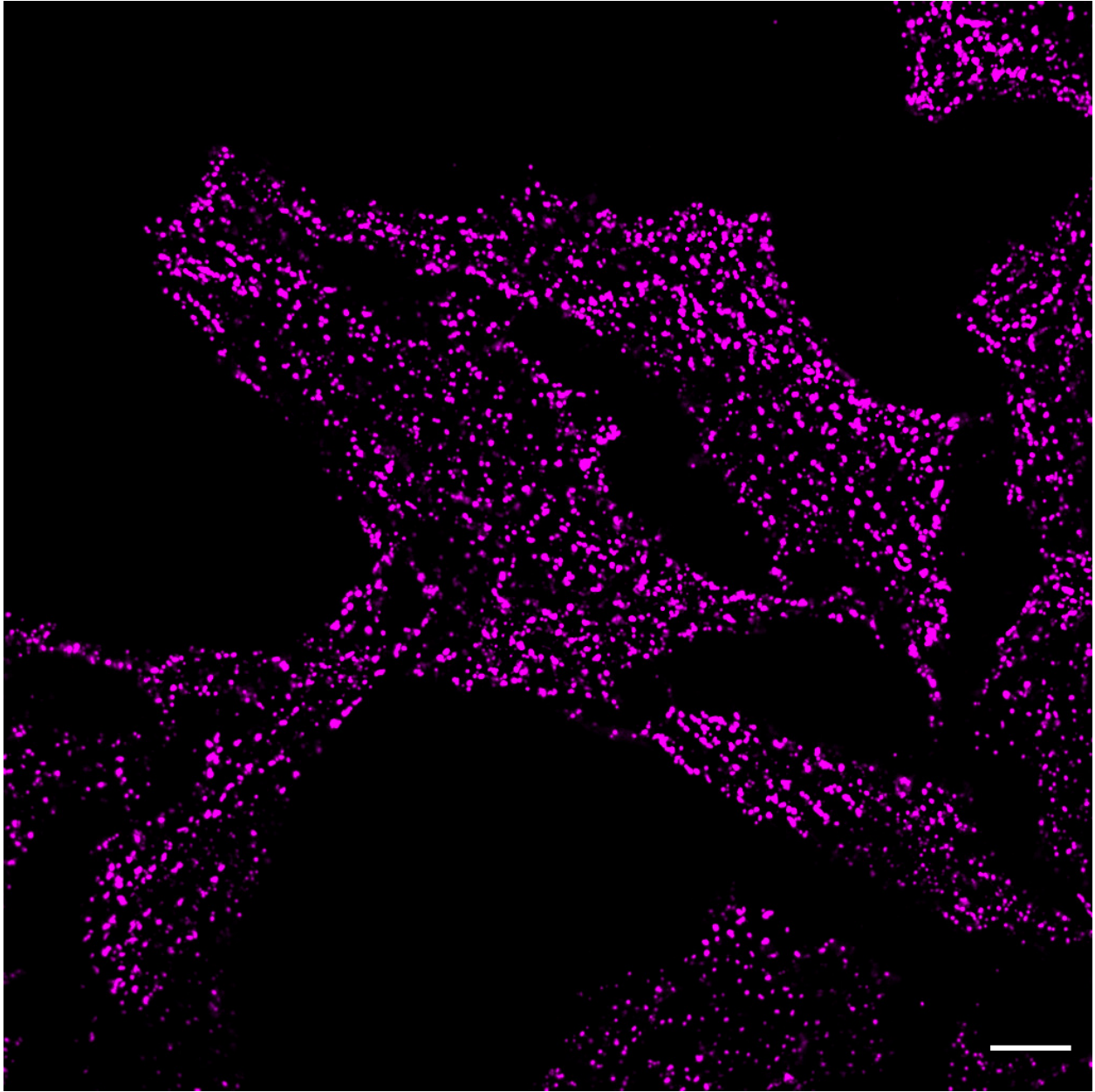


Figure S23. A confocal fluorescence micrograph of HeLa cells. The focal plane is set close to the bottom of the dish. Scale bar: 10 μm .

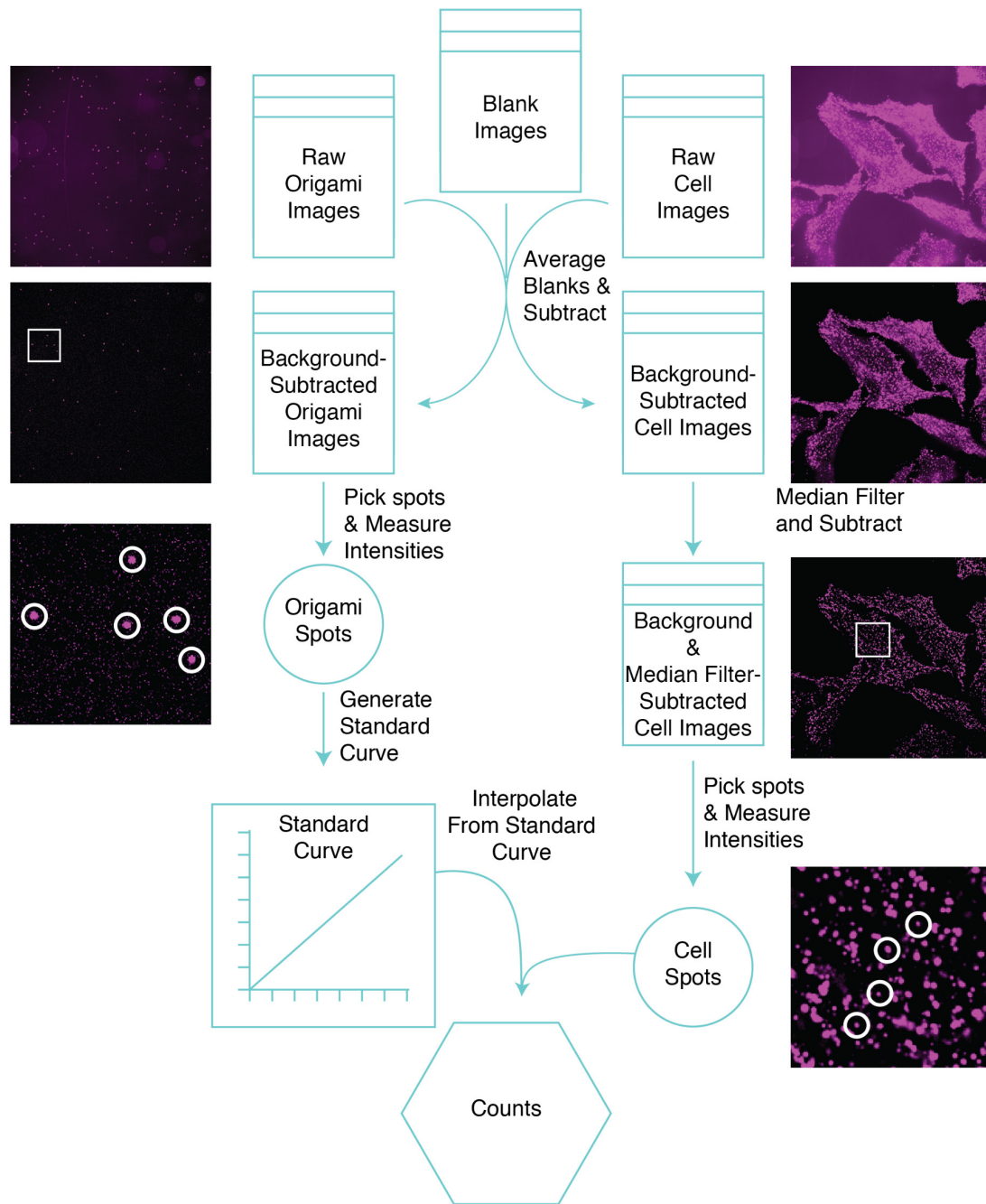


Figure S24. Image processing pipeline for SiR labeling. Background from media and the dish was approximated from empty dishes (blank images), and subtracted from all images containing SiR standards or HeLa cells. SiR puncta in DNA-origami images were picked using a custom TrackMate script, and used to construct the calibration curve. A background-subtracted image of cells was median filtered, and was subtracted from the cell images. CLC-SiR spots in cells were then picked manually (circled in sample images). CLC-SiR intensities were then converted to molecule number using the calibration curve.

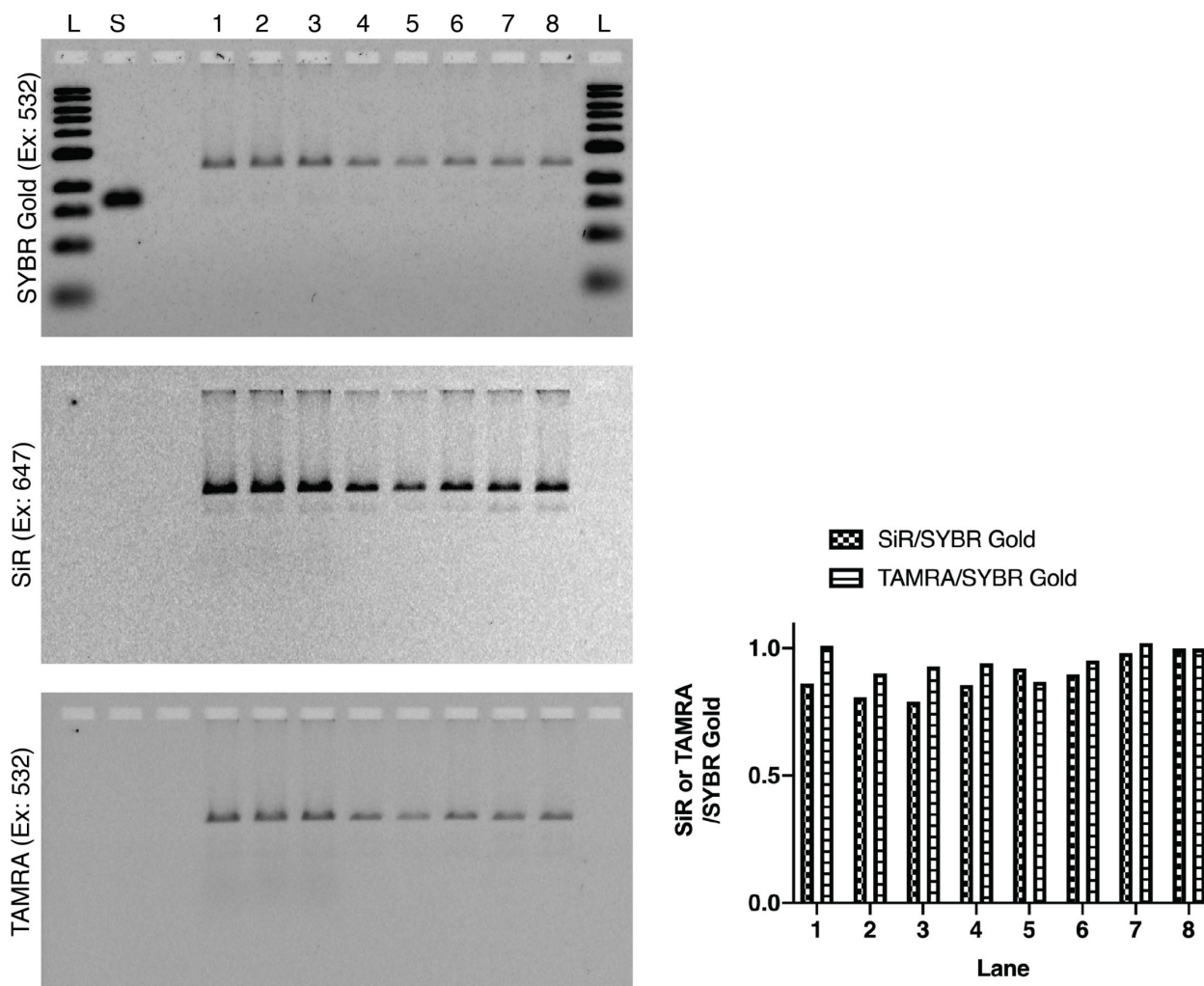


Figure S25. Stability of DNA-origami standards in imaging media. A dimeric-6hb-based SiR standard bearing 20 copies of SiR and 36 copies of TAMRA were subjected to media and temperatures simulating live-cell imaging conditions and run on an agarose gel. The media and temperature conditions were as follows: 1: Regular DMEM (Gibco, 21063-029, contains ~1 mM Mg^{2+}), 1hr @ 37°C; 2: DMEM + 2 mM $MgCl_2$, 1hr @ 37°C; 3: DMEM + 10 mM $MgCl_2$, 1hr @ 37°C; 4: Regular LCIS (Thermo Fisher, pH 7.4, A14291DJ, contains ~1 mM Mg^{2+}), 1hr @ 37°C; 5: LCIS + 2 mM $MgCl_2$, 1hr @ 37°C; 6: LCIS + 10 mM $MgCl_2$, 1hr @ 37°C; 7: 1×TE + 10 mM $MgCl_2$, 1hr @ 37°C; 8: 1×TE + 10 mM $MgCl_2$, RT (reference). SiR, TAMRA, and SYBR Gold intensities were measured using ImageJ and the ratios of SiR and TAMRA to SYBR gold are shown on the right (bar chart normalized to lane 8). Importantly, there was no indication of structural damage or fluorescence loss in LCIS or DMEM, regardless of the concentration of Mg^{2+} (1–10 mM), or whether structures were heated to 37°C, supporting the reliability of our DNA-origami brightness standards under live-cell imaging conditions.

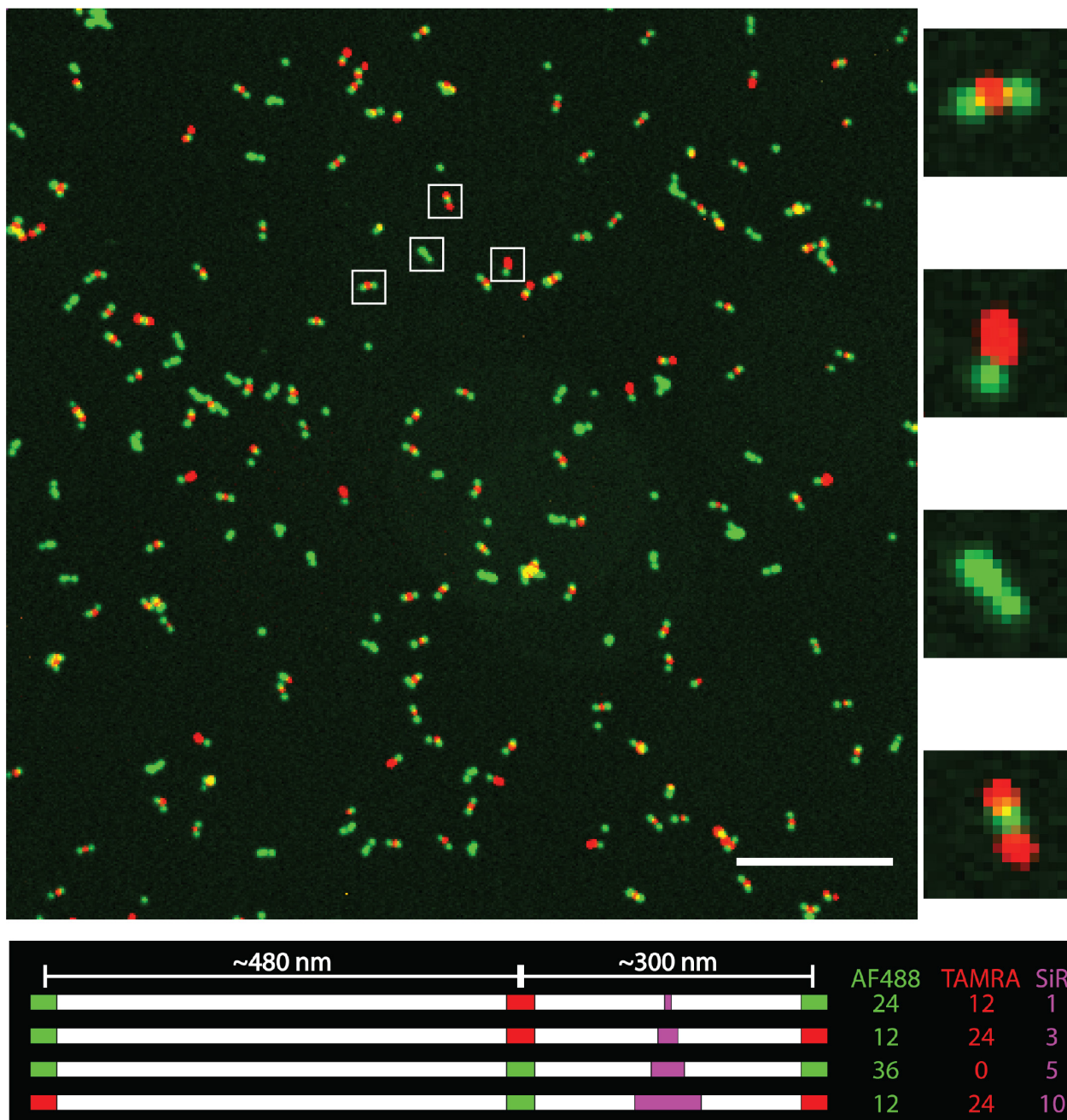


Figure S26. Multiple DNA-origami barcodes imaged together. Different DNA-origami 6hb structures (designed to display 1–10 SiR molecules) with distinct barcodes were mixed and imaged in 1× TE + 10 mM MgCl₂ using a TIRF microscope. DNA structures were fixed on a glass coverslip *via* biotin-streptavidin binding. Each imaging standard species is readily distinguishable from the image, which could enable multiplexed imaging. Pseudo-colors: Alexa Fluor 488 (green) and TAMRA (red). Scale bar: 10 μm.

Supplementary Tables

Table S1: Handle and antihandle sequences

Name	Sequence (5'-3')
Outer 2	<u>CTTCACACCACACTCCATCTA</u>
Inner 1	<u>AAATTATCTACCACAACCTCAC</u>
handle ix	<u>ACCTACTAACATAATCATCAC</u>
Non ATG 1 handle	<u>CGGTTGTA CTGTGACCGATTC</u>
Anti Outer 2	<u>TAGATGGAGTGTGGTGTGAAG</u>
Anti Inner 1	<u>GTGAGTTGTGGTAGATAATTT</u>
anti-handle ix	<u>GTGATGATTATGTTAGTAGGT</u>
Non-ATG 1 antihandle	<u>GAATCGGTCACAGTACAACCG</u>
5'Alkyne-anti Inner 1	<u>/5Hexynyl/GTGAGTTGTGGTAGATAATTT</u>
5' Biotin Non-ATG 1	<u>/5Biosq/GAATCGGTCACAGTACAACCG</u>
3'AF488-anti Inner 1	<u>GTGAGTTGTGGTAGATAATTT/3AlexF488N/</u>
5' AF488-anti handle ix	<u>/5Alex488N/TGTGATGATTATGTTAGTAGGT</u>
5' TAMRA-anti handle ix	<u>/56-TAMN/GTGATGATTATGTTAGTAGGT</u>
5' TAMRA-anti outer 2	<u>/56-TAMN/TAGATGGAGTGTGGTGTGAAG</u>
5' AF647-anti outer 2	<u>/5Alex647N/TAGATGGAGTGTGGTGTGAAG</u>

Table S2: Linker DNA strands used in dimers

Name	Sequence (5'-3')
LD1.1	CATTGCATGCCTGCGGAATTAGAGCCAGAAAGGTGAATTATC
LD1.2	CCAGTGCCAAGCGATTTGAAATACCGACAGAAAAAGCCTGTT
LD1.3	ACCGTCACCGACCCGAATCATAATTA CTCTCGTGTGATAAATAA
LD1.4	GGTTGAGCCATTTGAGGTCGACTCTAGATTGTA AACGACGG
LD1.5	GGCGTTAAATAACATCCCAGTCACGACGCCTTTGATAGCGAG
LD1.6	AAGAATAAACACCGGCTTTTGC GGGATCTGCAGGGAGTTAAA

Table S3: DNA-origami-assisted quantitative fluorescence microscopy methods

	DNA-origami-based brightness standards		DNA-origami-calibrated STORM	DNA-PAINT-based quantification
Reference	18,19,20	This work	21	22,23
Dynamic range	1-132	5-200	1-35	1-50
Speed	Fast		Slow	Slow
Fluorophore and conjugation	DNA-conjugated cell-impermeable organic dyes	Fluorescent proteins and cell-permeable organic dyes	Antibody-conjugated organic dyes	DNA-conjugated organic dyes
Biological sample?	<i>In vitro</i> nucleic acid detection	Live cells	Fixed cells	Fixed cells: require antibody-conjugated DNA strands
Difficulty	Low	Low	High	High
Acquisition time	Typically <1 sec	1 sec	~1 hour	0.4-2.8 hours

Table S4: Imaging parameters

	mEGFP-labeled samples		SiR-labeled samples		
Microscope	Leica DMI8 wide-field inverted microscope		Nikon TiE inverted confocal with Yokogawa CSU-W1 spinning disk (50 μ m disk pattern)		
Light source	Lumencor SpectraX (LED)		Multiple lasers		
Objective	HC Plan Apochromat 100 \times DIC, N.A. 1.4, W.D. 90 μ m, No: 11506381		CFI Plan Apochromat Lambda 60x/1.4 Oil, W.D. 0.13 mm, No: MRD01605		
Camera	Andor iXon Ultra888 EMCCD		Andor iXon Ultra888 EMCCD		
Fluorophore	mEGFP	AF647	SiR	AF488	TAMRA
Excitation wavelength (nm)	470/24	640/30	647	488	561
Excitation filter (nm)	470/40	620/60	N.A.	N.A.	N.A.
Dichroic mirror (nm)	495	660	405/488/561/647		
Emission filter (nm)	525/50	700/75	700/75	525/36	605/70
Excitation power	196 mW, 50%	231 mW, 10%	190 mW*, 70%	130 mW*, 40%	130 mW*, 40%
Exposure time (s)	1	1	1	1	1

*Laser power measured at fiber tip.

Supplementary References

- (1) Douglas, S. M.; Marblestone, A. H.; Teerapittayanon, S.; Vazquez, A.; Church, G. M.; Shih, W. M. Rapid Prototyping of 3D DNA-Origami Shapes with CaDNAno. *Nucleic acids research* **2009**, *37* (15), 5001–5006. <https://doi.org/10.1093/nar/gkp436>.
- (2) Douglas, S. M.; Dietz, H.; Liedl, T.; Högberg, B.; Graf, F.; Shih, W. M. Self-Assembly of DNA into Nanoscale Three-Dimensional Shapes. *Nature* **2009**, *459* (7245), 414–418. <https://doi.org/10.1038/nature08016>.
- (3) Stahl, E.; Martin, T. G.; Praetorius, F.; Dietz, H. Facile and Scalable Preparation of Pure and Dense DNA Origami Solutions. *Angewandte Chemie International Edition* **2014**, *53* (47), 12735–12740. <https://doi.org/10.1002/anie.201405991>.
- (4) Lin, C.; Perrault, S. D.; Kwak, M.; Graf, F.; Shih, W. M. Purification of DNA-Origami Nanostructures by Rate-Zonal Centrifugation. *Nucleic acids research* **2013**, *41* (2), e40–e40. <https://doi.org/10.1093/nar/gks1070>.
- (5) Lajoie, M. J.; Rovner, A. J.; Goodman, D. B.; Aerni, H.-R.; Haimovich, A. D.; Kuznetsov, G.; Mercer, J. A.; Wang, H. H.; Carr, P. A.; Mosberg, J. A.; Rohland, N.; Schultz, P. G.; Jacobson, J. M.; Rinehart, J.; Church, G. M.; Isaacs, F. J. Genomically Recoded Organisms Expand Biological Functions. *Science* **2013**, *342* (6156), 357–360. <https://doi.org/10.1126/science.1241459>.
- (6) Amiram, M.; Haimovich, A. D.; Fan, C.; Wang, Y.-S.; Aerni, H.-R.; Ntai, I.; Moonan, D. W.; Ma, N. J.; Rovner, A. J.; Hong, S. H.; Kelleher, N. L.; Goodman, A. L.; Jewett, M. C.; Söll, D.; Rinehart, J.; Isaacs, F. J. Evolution of Translation Machinery in Recoded Bacteria Enables Multi-Site Incorporation of Nonstandard Amino Acids. *Nature biotechnology* **2015**, *33* (12), 1272–1279. <https://doi.org/10.1038/nbt.3372>.
- (7) Presolski, S. I.; Hong, V. P.; Finn, M. G. Copper-Catalyzed Azide-Alkyne Click Chemistry for Bioconjugation. *Current protocols in chemical biology* **2011**, *3* (4), 153–162. <https://doi.org/10.1002/9780470559277.ch110148>.
- (8) Lin, C.; Jungmann, R.; Leifer, A. M.; Li, C.; Levner, D.; Church, G. M.; Shih, W. M.; Yin, P. Submicrometre Geometrically Encoded Fluorescent Barcodes Self-Assembled from DNA. *Nat Chem* **2012**, *4* (10), 832–839. <https://doi.org/10.1038/nchem.1451>.
- (9) Mangiameli, S. M.; Veit, B.T.; Merrikh, H.; Wiggins, P. A. The Replisomes remain spatially proximal throughout the Cell Cycle in Bacteria. *PLOS Genetics*. **2017**, *13*, e1006582. <https://doi.org/10.1371/journal.pgen.1006582>.
- (10) Ducret, A.; Quardokus, E. M.; Brun, Y. V. MicrobeJ, a Tool for High Throughput Bacterial Cell Detection and Quantitative Analysis. *Nat. Microbiol.* **2016**, 1–7. <https://doi.org/10.1038/nmicrobiol.2016.77>.

- (11) *GraphPad Prism* version 8.4.3 for macOS; GraphPad Software: San Diego, CA USA, 2020.
- (12) Cong, L.; Ran, F. A.; Cox, D.; Lin, S.; Barretto, R.; Habib, N.; Hsu, P. D.; Wu, X.; Jiang, W.; Marraffini, L. A.; Zhang, F. Multiplex Genome Engineering Using CRISPR/Cas Systems. *Science* **2013**, *339* (6121), 819–823. <https://doi.org/10.1126/science.1231143>.
- (13) Takakura, H.; Zhang, Y.; Erdmann, R. S.; Thompson, A. D.; Lin, Y.; McNellis, B.; Rivera-Molina, F.; Uno, S.; Kamiya, M.; Urano, Y.; Rothman, J. E.; Bewersdorf, J.; Schepartz, A.; Toomre, D. Long Time-Lapse Nanoscopy with Spontaneously Blinking Membrane Probes. *Nature Biotechnol.* **2017**, 773–780. <https://doi.org/10.1038/nbt.3876>.
- (14) Saffarian, S.; Cocucci, E.; Kirchhausen, T. Distinct Dynamics of Endocytic Clathrin-Coated Pits and Coated Plaques. *PLOS Biology* **2009**, *7* (9), e1000191-18. <https://doi.org/10.1371/journal.pbio.1000191>.
- (15) Gan, L.; Chao, T.-C.; Camacho-Alanis, F.; Ros, A. Six-Helix Bundle and Triangle DNA Origami Insulator-Based Dielectrophoresis. *Analytical Chemistry* **2013**, *85* (23), 11427–11434. <https://doi.org/10.1021/ac402493u>.
- (16) Milles, S.; Tyagi, S.; Banterle, N.; Koehler, C.; VanDelinder, V.; Plass, T.; Neal, A. P.; Lemke, E. A. Click Strategies for Single-Molecule Protein Fluorescence. *J. Am. Chem. Soc.* **2012**, *134* (11), 5187–5195. <https://doi.org/10.1021/ja210587q>.
- (17) *The MathWorks MATLAB* version 9.8.0.1359463 (R2020a) Update 1 for macOS; The MathWorks, Inc.: Natick, MA USA, 2020.
- (18) Schmied, J. J.; Gietl, A.; Holzmeister, P.; Forthmann, C.; Steinhauer, C.; Dammeyer, T.; Tinnefeld, P. Fluorescence and Super-Resolution Standards Based on DNA Origami. *Nature methods* **2012**, *9* (12), 1133–1134. <https://doi.org/10.1038/nmeth.2254>.
- (19) Schmied, J. J.; Raab, M.; Forthmann, C.; Pibiri, E.; Wünsch, B.; Dammeyer, T.; Tinnefeld, P. DNA Origami-Based Standards for Quantitative Fluorescence Microscopy. *Nature protocols* **2014**, *9* (6), 1367–1391. <https://doi.org/10.1038/nprot.2014.079>.
- (20) Woehrstein, J. B.; Strauss, M. T.; Ong, L. L.; Wei, B.; Zhang, D. Y.; Jungmann, R.; Yin, P. Sub-100-Nm Metafluorophores with Digitally Tunable Optical Properties Self-Assembled from DNA. *Science Advances* **2017**, *3* (6). <https://doi.org/10.1126/sciadv.1602128>.
- (21) Znacchi, F. C.; Manzo, C.; Alvarez, A. S.; Derr, N. D.; Garcia-Parajo, M. F.; Lakadamyali, M. A DNA Origami Platform for Quantifying Protein Copy Number in Super-Resolution. *Nature methods* **2017**, *14* (8), 789–792. <https://doi.org/10.1038/nmeth.4342>.

(22) Jungmann, R.; Avendaño, M. S.; Dai, M.; Woehrstein, J. B.; Agasti, S. S.; Feiger, Z.; Rodal, A.; Yin, P. Quantitative Super-Resolution Imaging with QPAINT. *Nature methods* **2016**, *13* (5), 439–442. <https://doi.org/10.1038/nmeth.3804>.

(23) Stein, J.; Stehr, F.; Schueler, P.; Blumhardt, P.; Schueder, F.; Mücksch, J.; Jungmann, R.; Schwille, P. Towards Absolute Molecular Numbers in DNA-PAINT. *Nano Letters* **2019**, *19* (11), 8182–8190. <https://doi.org/10.1021/acs.nanolett.9b03546>.